NOVA SCHOOL OF
SCIENCE & TECHNOLOGY

DEPARTMENT OF MATERIALS SCIENCE

BÁRBARA DE LIMA SIEIRA

BSc in Micro and Nanotechnology Engineering

NANOSTRUCTURING GOLD ELECTRODES VIA ANODIZATION FOR ELECTROCHEMICAL BIOSENSORS

MASTER IN MICRO AND NANOTECHNOLOGY ENGINEERING

NOVA University Lisbon

October, 2023

NOVA SCHOOL OF SCIENCE & TECHNOLOGY

DEPARTAMENT OF MATERIALS SCIENCE

NANOSTRUCTURING GOLD ELECTRODES VIA ANODIZATION FOR ELECTROCHEMICAL BIOSENSORS

Bárbara de Lima Sieira
BSc in Micro and Nanotechnology Engineering

Adviser: Irene Taurino
Full Professor, KU Leuven

Co-advisers: Joana Vaz Pinto
Full Professor, NOVA University Lisbon

Examination Committee:

Chair: Dr. Rui Alberto Garção Barreira do Nascimento Igreja
Full Professor, FCT-NOVA

Rapporteurs: Dra. Rita Maria Mourão Salazar Branquinho
Full Professor, FCT-NOVA

Adviser: Dra. Irene Taurino,
Full Professor, KU Leuven

MASTER IN MICRO AND NANOTECHNOLOGY ENGINEERING

NOVA University Lisbon

October, 2023

NANOSTRUCTURING GOLD ELECTRODES FOR GLUCOSE DETECTION VIA ANODIZATION FOR ELECTROCHEMICAL BIOSENSORS

Para a minha família,

ACKNOWLEDGEMENTS

Finishing this thesis marks a significant milestone in my life's path, a result of years of hard work and unwavering dedication. Naturally, I am filled with immense joy and a sense of accomplishment as I conclude this chapter, and I wish to express my heartfelt gratitude to all those who have been by my side throughout this journey.

I am profoundly grateful to the individuals and organizations who have supported and guided me throughout my journey in completing this master's thesis. Their contributions have been instrumental in the success of this research endeavour.

First, I would like to extend my heartfelt appreciation to my thesis advisors, Prof. Irene Taurino and Prof. Joana Vaz Pinto. Their unwavering commitment, expert guidance, and continual encouragement propelled this research from inception to completion. Their dedication to my academic and professional growth has been invaluable.

I am indebted to NOVA University and KU Leuven for giving me the experience of living abroad while working on this amazing project with the best team. Their belief in the potential of this work has allowed me to focus my energy and resources on contributing to the field of engineering. Also, thank you for their insightful feedback and constructive criticism which improved the quality and depth of this thesis.

I would like to recognize and thank my research collaborators, Filippo Franceschini, Nurul Rusli, Catarina Fernandes, and Ruben Van den Eeckhoudt, for their contributions, shared expertise, and valuable discussions that enhanced the scope and impact of this research.

The unwavering support and encouragement of my family and friends have been a source of inspiration throughout my academic journey. Their patience and understanding during the demanding phases of this research were indispensable.

I extend my gratitude to the faculty and staff at NOVA Science of Technology, especially the Materials Department, for providing a conducive academic environment and access to necessary resources.

Additionally, I wish to thank all those individuals who played a role, whether small or large, in helping me with equipment, software, and access to facilities during this research.

Lastly, I express my sincere thanks to every source of inspiration that motivated me on this challenging yet rewarding academic voyage.

Thank you all for being a part of this remarkable journey.

"Difficult roads often lead to beautiful destinations."

Zig Ziglar

ABSTRACT

Continuous glucose monitors (CGMs) are indispensable devices for the detection and management of diabetes, a condition that significantly affects the lives of millions of patients. The early identification of diabetes plays a pivotal role in preserving patient well-being and curbing the escalating costs associated with treatment.

Traditionally, glucose sensing methods have encountered limitations in terms of precision, sensitivity, and response time due to their reliance on enzymes as receptors. To tackle these challenges, researchers have shifted their focus toward the development of advanced non-enzymatic electrochemical glucose sensors. In this pursuit, the creation and utilization of an efficient electrode emerge as a critical element. Among various materials under consideration, gold electrodes have garnered considerable attention owing to their exceptional conductivity, stability, biocompatibility, and electrocatalytic capabilities for glucose in neutral pH conditions—vital prerequisites for continuous monitoring.

Anodization, a controlled electrochemical oxidation process, presents a unique opportunity for tailoring the surface characteristics of gold electrodes. This enables the fine-tuning of sensitivity, selectivity toward glucose, and signal stability in media containing physiological chloride concentrations. By meticulously optimizing anodization parameters like applied potential, electrolyte concentration, and reaction time, one can engineer nanostructured gold surfaces with enhanced attributes.

In this study, some differences in crystallographic orientations, morphology, and glucose sensing were detected. It highlights the influence of chloride ions on nanostructured electrodes, underscores the significance of a meticulously optimized cleaning protocol for reliable measurements, and underscores the role of crystallographic planes in sensitivity concerning the electrooxidation potential of glucose.

Moreover, the versatility of this technique is showcased as it can be applied to roughened microelectrodes decreasing fourteen times the impedance of the initial value, opening up an expansive research domain. The anodized samples exhibit a good sensitivity ($(30 \pm 5)\ \mu A/cm^2 \cdot mM$) to glucose at lower potentials (0.05 V) compared to unmodified gold electrodes ($(41 \pm 4)\ \mu A/cm^2 \cdot mM$ at 0.3 V). This innovation holds substantial promise for the development of energy-efficient, sensitive, and selective electrochemical sensors for glucose detection.

Keywords: Nanostructured gold, Anodization, Crystallographic planes, Low potential non-enzymatic glucose sensing.

RESUMO

Os monitores contínuos de glucose (MCGs) são dispositivos indispensáveis para a deteção e gestão da diabetes, uma condição que afeta significativamente a vida de milhões de doentes. A identificação precoce da diabetes desempenha um papel crucial na preservação do bem-estar do doente e na contenção dos crescentes custos associados ao tratamento.

Tradicionalmente, os métodos de deteção de glucose têm enfrentado limitações em termos de precisão, sensibilidade e tempo de resposta devido à sua dependência de enzimas como recetores. Para enfrentar estes desafios, os investigadores têm direcionado o seu foco para o desenvolvimento de sensores avançados de glucose eletroquímicos não enzimáticos. Nesta busca, a criação e utilização de um elétrodo eficiente emergem como um elemento crítico. Entre diversos materiais em consideração, os elétrodos de ouro têm recebido considerável atenção devido à sua excecional condutividade, estabilidade, biocompatibilidade e capacidades eletrocatalíticas para a glucose em condições de pH neutro, pré-requisitos vitais para monitorização contínua.

A anodização, um processo controlado de oxidação eletroquímica, apresenta uma oportunidade única para ajustar as características de superfície dos elétrodos de ouro. Isso permite o ajuste fino da sensibilidade, seletividade para a glucose e estabilidade do sinal em meios contendo concentrações fisiológicas de cloreto. Através da otimização meticulosa dos parâmetros de anodização, como potencial aplicado, concentração do eletrólito e tempo de reação, é possível criar superfícies de ouro nanoestruturadas com atributos aprimorados.

Neste estudo, foram detetadas algumas diferenças nas orientações cristalográficas, morfologia e deteção de glucose. Isso destaca a influência dos iões cloreto em elétrodos nanoestruturados, enfatiza a importância de um protocolo de limpeza meticulosamente otimizado para medições confiáveis e sublinha o papel dos planos cristalográficos na sensibilidade em relação ao potencial de eletroxidação da glucose.

Além disso, a versatilidade desta técnica é demonstrada, pois pode ser aplicada a microeletrodos rugosos, reduzindo catorze vezes a impedância do valor inicial, abrindo um amplo campo de pesquisa. As amostras anodizadas exibem boa sensibilidade ($(30 \pm 5)\ \mu A/cm^2 \cdot mM$) para a glucose em potenciais mais baixos (0.05 V) em comparação com os elétrodos de ouro não modificados ($(41 \pm 4)\ \mu A/cm^2 \cdot mM$ a 0.3 V). Esta inovação possui promissoras para o desenvolvimento de sensores eletroquímicos para deteção de glucose eficientes em energia, sensíveis e seletivos.

Palavras-chave: Ouro nanoestruturado, Anodização, Planos cristalográficos, Deteção de glucose não enzimática a baixo potencial

CONTENTS

LIST OF FIGURES

LIST OF TABLES

GLOSSARY

Cycle	Signal read when a potential is applied at the working electrode in both forward and reverse directions.
Electrolyte	A liquid or gel which contains ions and can be decomposed by electrolysis.
Oxidizing	Substance in a redox chemical reaction that gains or "accepts"/"receives" an electron from a reducing agent.
Scan rate	The rate of voltage changes over time during each of these phases.
Step size	Parameter which combines with the scan range on any given cycle to determine the number of data points.
Threshold	Amount, level or limit on a certain scale.

ACRONYMS

3D	3 Dimensional
BNC	Bayonet Neill–Concelman
CE	Counter Electrode
CV	Cyclic Voltammetry
CA	Chronoamperometry
DI	Deionized Water
DNA	Deoxyribonucleic Acid
ESA	Electrochemical Surface Area
FM	Floating Mode
IPA	Isopropanol
IUPAC	International Union of Pure and Applied Chemistry
LSV	Linear Sweep Voltammetry
NPG	Nanoporous Gold
Ox	Oxidizing Agent
PB	Phosphate Buffer
PBS	Phosphate Buffer Saline
PCB	Printed Circuit Board
POC	Point-of-Care
PR	Photoresist
R&D	Research and Development
RE	Reference Electrode
Red	Reducing Agent
SC	Short-circuit
SEM	Scanning Electron Microscope
WE	Working Electrode
XRD	X-ray Diffraction

SYMBOLS

$\mathbf{C_{DL}}$	Double-layer capacitance [F]
$\mathbf{C_{par}}$	Parasitic capacitance [F]
$\mathbf{f_c}$	Crossover frequency [Hz]
j	Current [A]
$\mathbf{R_{sol}}$	Solution resistance [Ω]
v	Scan rate in [V/s]
$\mathbf{V_{PP}}$	Peak-to-peak voltage [V]
ω	Angular frequency

MOTIVATION

The motivation for this thesis was to explore the potential of the anodization technique to enhance the performance of gold electrodes for non-enzymatic glucose sensing applications. The market for glucose sensors has grown significantly, now holding about 85% of the global biosensor industry. The blood glucose monitoring device market was valued at USD 11.71 billion globally in 2021, and it is projected to grow to USD 27.2 billion by 2026. As this happens, the scientific community has been inspired to develop cutting-edge glucose sensing products by the increasing demand for glucose sensors. By nanostructuring gold electrodes, it is possible to sense glucose at lower potentials which can result in a highly specific sensor. Besides this project bases on a non-enzymatic sensor, meaning there is no need to immobilize any biomolecule on the electrode surface, facilitating this process and also decreasing the productions costs.

Anodization, a controlled electrochemical oxidation process which offers a unique opportunity to swiftly modify the surface properties of gold electrodes in one step without the use of harsh chemicals, thereby improving their sensitivity, selectivity, and stability. By carefully optimizing the anodization parameters, such as applied potential, electrolyte composition, and reaction time, it is possible to tailor the surface morphology and create nanostructured gold surfaces with enhanced electrooxidation capabilities towards glucose.

The development of highly sensitive and reliable glucose sensors is of paramount importance in the field of diabetes management. Anodization can create nanostructured gold surfaces, leading to increased surface area and improved mass transport properties. This, in turn, can enhance the sensitivity of the glucose sensor, enabling accurate and real-time glucose measurements.

This technique also allows to tailor the crystallographic characteristics of the gold which could enable an enhanced selectivity and specificity of the glucose sensor. Besides, it can produce nanoporous gold (NPG) electrodes that can exhibit improved stability and resistance to fouling, ensuring the long-term performance and reliability of the glucose sensor. This is particularly vital for continuous glucose monitoring applications, where prolonged sensor lifetimes are desired.

Besides these points, anodization can be compatible with microfabrication processes, facilitating the integration of the anodized gold electrodes into miniaturized and implantable glucose sensor devices. This opens up possibilities for the development of wearable and implantable glucose monitoring systems, offering improved convenience and quality of life for diabetes patients or other medical issues.

In conclusion, the anodization of gold electrodes holds immense potential for advancing glucose sensing technology. By harnessing the unique properties and controllable surface modifications enabled by anodization, this project aims to contribute to the development of highly sensitive, selective, and stable glucose sensors. Through this research, the team aspires to make significant strides towards improving diabetes management and ultimately enhancing the well-being of individuals living with diabetes.

1

INTRODUCTION

1.1. General overview of nanostructured gold for electrochemical biosensors

The early-stage detection of diseases can play an important role in both, patient health and the reduction of healthcare costs [1]. Over the past five decades, there has been an outstanding improvement in electrochemical sensors to enrich the quality of human life [2]. Researchers' main focus is based on achieving a continuous and real-time measurement of clinically relevant molecules and thus developing ad-hoc implantable, wearable or point-of-care (POC) devices [2]. Until now, different types of electrochemical devices have been developed to reduce the impact of these societal issues [3].

Electrochemistry itself is considered a branch of chemistry that makes a bridge between chemical and electrochemical effects. It analyzes a signal generated from reactions that involve electron transfer between the chemical in solution and the electrode surface. As already reported, the flow of electrons is linked with the redox reactions and is usually described as follows,

$$Ox + ne^- \rightleftharpoons Red, \qquad [1]$$

where Ox is the oxidizing component and Red is the reduced one.

The dynamic force, that leads to an electron exchange, is the voltage difference applied between the electrode where the electron exchange takes place (working electrode) and a reference electrode.

Thanks to extensive research conducted over the past few decades, the researchers engender the monitoring and understanding of the chemical mechanisms behind the reactions of some biomolecules. This comprehensive understanding has paved the way for the creation of electrochemical biosensors, which possess the capability to accurately detect these biomolecules. Moreover, by methodically controlling and adjusting certain parameters of the reactions, these biosensors can be adapted for diverse applications across various fields.

According to the IUPAC recommendation (1999), an electrochemical biosensor is categorized as an integrated device that provides specific quantitative or semi-quantitative analytical data. The data is collected from a biological sensing component (receptor) that entered in direct spatial contact with a transductor element. Both elements can achieve direct conversion of a biological signal into an electrical one [4].

These groups of biosensors can be divided into four distinctive categories. The reaction can produce a measurable current (*amperometric*), a determinate potential or charge accumulation (*potentiometric*), a change in current as a function of the applied potential (*voltammetric*), and also can sense an impedance signal (*impedimetric*) [3][5][6].

In 1962, the first device that consisted of an enzyme electrode to detect glucose was developed. This was introduced to the market by Leland C. Clark and was only commercially available in 1975 [7]. The purpose of the device was to detect glucose from a blood sample in diabetes patients. Later, in 1969, Guilbault and Montalvo developed a different biosensor which measured urea concentration on glass electrodes immobilized with urease [8].

As expected, these publications had a huge impact on research, opening a great study topic. Since then, electrochemical transducers have been using different biomolecules, such as DNA, enzymes, and antibodies as recognition components. Currently, they represent the majority of biosensors used for detection in the medical, environmental, and food industries [9].

As mentioned before, the core of the operation of electrochemical biosensors is the conversion of biochemical events into electrical signals. For this, an electrode is a crucial component which has been used as a firm support for the immobilization of biomolecules and the flow of electrons [10].

In recent years, nanotechnology has been revolutionizing the biosensors sector as nanomaterial-modified electrodes are being used as a sensing platform for this type of device [8]. These materials present different structures on the scale of nanometers, usually between 1 and 100 nm. They have revealed some new properties when compared to bulk materials, becoming more abundant than ever [11]. These properties normally depend on some features such as the size, shape, and morphology of the nanostructure which can be tuned to achieve different final results [12].

Among all the porous metallic films produced until now, gold has some particular features as its chemical stability and distinctive surface chemistry [13]. In modern industry, gold was broadly used for electronics as connectors due to its great conductivity and corrosion resistance [14]. Nowadays, there is a huge interest towards gold chemistry and novel nanofabrication methods to tailor gold properties ranging from electrical and electrochemical and chemical stability in various media, opening up new R&D opportunities [13] [14]. The fact that this material exhibits a large surface area makes it suitable for high-performance devices, in other words, it achieves a great analytical sensitivity by increasing the reactant loading capacity and mass transport [15].

For the last five decades, this porous gold has been employed in diverse areas such as electronics, photonics, and medicine [16]. It can be produced following various approaches namely, dealloying, electrodeposition, self-assembly, anodization, and some 3D printing techniques (such as nanoimprinting lithography and laser imprint technology) [13] [17].

Here, the focus will be on anodization as a simple, fast, and user-friendly technique to produce porous gold. This technique has gained a lot of interest within the research community since it showed the roughening of a smooth gold electrode to a nanostructured one. Until the moment, it already efficiently produced nanoporous gold (NPG) that was able to sense glucose [18], dopamine [19], and cocaine [20], among many other molecules.

1.2. Anodization of gold

In the last decades, anodization has generated considerable attention from researchers as a new method to synthesize porous materials with structures and pore sizes of a few nanometers. This technique consists on the application of constant voltage or current between the anode and cathode. Electrode reactions (oxidation and reduction) take place, and combined with field-driven ion diffusion, lead to the formation of an oxide layer on the anode surface (Figure 1) [21].

Anodic oxidation was first observed by Buff in late 1920 who exploited it for industrial-scale application, for example, to protect aluminium fragments from corrosion. In the 1960s this technique was widely studied to improve implant osseointegration and since then it has not only been used to improve the corrosion resistance but also to dye and enhance the wear resistance of ductile metals [21] [22].

Currently, anodization is being utilized as a tool to fabricate self-organized nanostructures by oxidation of metal electrodes that can be applied in, for example, electrochemical biosensors for the measurement of clinically relevant molecules [23] [24].

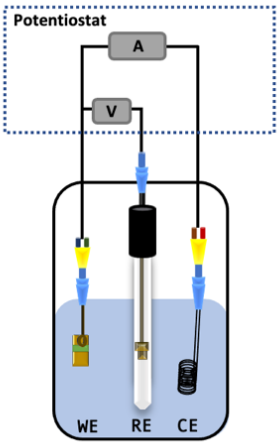

Figure 1 - Schematic of anodization set-up: three-electrode cell system.

As schematized, anodization is an electrochemical process where a metal material is immersed in an electrolyte solution in a three-electrode system [20]. The reaction of interest, in this case, the oxidation and reduction of gold occurs at the working electrode (WE). This electrode will have its potential either to be scanned or to be held constant to perform the redox reactions. The reference electrode (RE) should provide a well-defined redox couple which is used to compare against what is occurring at the working and counter electrodes. Finally, the counter electrode (CE) completes the circuit within the full electrochemical cell.

This electrochemical reaction can happen in both two-electrode or three-electrode cells. The two-electrode cell system is based on a WE and a RE, which has a known potential. In this set-up, the current is flowing between both electrodes. Since the electrolyte solution presents an intrinsic resistance, R_s, when the redox reactions occur, the current flowing is limited, causing a voltage drop in the electrolyte. Besides, the RE has a well-defined potential which is affected by the change of voltage happening in the media compromising the stability of the RE material.

As this happens, a three-electrode system was chosen for this project. In this cell system, the current flows between the WE and the CE, avoiding the current collection caused by the RE. The main function of the CE is to avoid the potential drop previously explained. Even though by placing the RE close to the WE, as represented in Figure 1, some fraction of this loss is still measured, since it is so little, a modern potentiostat is capable of compensating for this effect.

$$3AuCl_2^- \rightarrow AuCl_4^- + 2Au^* + 2Cl^- \qquad [2]$$

By applying an optimal potential to the system, the surface Au is roughened as a result of electrochemical dissolution – as reported by *Li et al.* – producing $AuCl_2^-$ and $AuCl_4^-$. $AuCl_2^-$ participates right away in disproportionation processes to create fresh Au* atoms. Then, accumulated Au* atoms are placed on the rough Au surface, creating the NPG structure [18].

For most applications, the electrolytes that have shown the ability to efficiently produce a nanostructure were KCl, HCl, H_2SO_4, citric, carboxylic, and oxalic acids [19] [25] [26]. However, the solutions containing chloride ions – as reported by *Li et. al* – have been shown as time-saving electrolytes. Even though carboxylic acids produced an efficient electrode roughening, the reaction is slow, taking more than one hour. As mentioned, according to the literature, HCl and KCl can anodize the electrode in considerably less time, in one and five minutes, respectively [18].

Au* atoms – Gold active atoms generated from the disprotonation processes on gold electrodissolution

However, the electrode materials used depend very much on the nature of the application [26-28]. The same

happens with the WE material selection, as this decision is based on the potential needed for the experiments and whether it is necessary to encourage or discourage species from adhering to surfaces to initiate redox reactions.

A well-efficient cleaning protocol of the WE has been shown as crucial before anodization – as reported by *Kim et al.* [26] and *Mie et al.* [18] - to ensure the electrode surface is free of any contamination. *Kim et al.* based the cleaning protocol on immersing the electrode in 0.1M phosphate buffer cycling 5 times the potential between -0.2 V and 1.2 V vs. Ag/AgCl. On the other hand, *Mie et al.* submerged the electrode in 0.5M sulfuric acid scanning a potential between -0.2 V and 1.6 V vs. Ag/AgCl [26] [18].

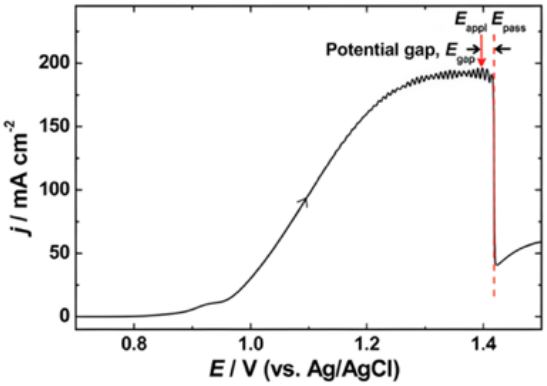

Figure 2 – Linear Sweep Voltammetry of the gold electrode in 1M KCl at a scan rate of 5 mV/s (Pt as CE and Ag/AgCl as RE) [18].

As illustrated in Figure 2, one of the reactions studied to optimize the anodization itself, begins with the electrochemical dissolution of the gold surface which leads to the production of chloride ions complexes. After that, in the linear sweep voltammetry recorded along the potentials 0.7 and 1.5 V vs Ag/AgCl, when the current reaches values between 1.3 and 1.4 V vs. Ag/AgCl, the reaction is controlled by the diffusion of these ions to the surface – as reported by *Kim et al.*– being defined as the plateau region. At the end of this region, the current generated drops off sharply which is an indicator for surface passivation (oxide layer formation). It has been demonstrated the anodization should occur at potentials immediately before the passivation. In this specific region, the gold present on the surface is constantly dissolved and the active gold is redepositing on the electrode surface [18].

The electrolyte pH also plays an important role in the roughening of the electrodes. As reported by *Kim et al.*, for neutral pH values an increase in the area was observed. For a pH above 8, the surface remained the same, suggesting higher pH is inefficient at dissolving Au [18]. At the same time, buffered solutions (1M KCl and 0.1M PB) have been shown to produce nanostructures with greater roughness than unbuffered ones (1M KCl only) [18].

NPG formation *via* anodization happens in two stages. The first one relies on the oxidation reaction where, as the name suggests, there is the change on the oxidation state of gold. In the second stage, the reduction reaction takes place – as *Saenz et al.* [19] and *Sukeri et al.* [27] reported - by recording a reverse scan, or – as reported by *Sadeghi et al.* [28] and *Tavakolli et al.* [20] – by immersing the WE in ascorbic acid, a low-cost and non-toxic reducing agent.

Until the moment, *Kim et al.*, *Mie et al.*, and *Saenz et al.* described anodization as a well-efficient technique to produce gold nanostructures for applications in sensing platforms, such as glucose, nicotinamide adenine dinucleotide (NAD^+), and dopamine biosensors.

Comparing their works (Table 1), the tunability of anodization has been proved. To produce a glucose sensor, a 2 mm gold wire is immersed in – as *Kim et al.* reported [18] – 1M KCl along with a platinum wire (*CE*) and Ag/AgCl (*RE*). By applying a constant voltage of 1.37 V for 400 seconds, this team obtained an NPG with a roughness factor (R_f) of 750, and a pore size of 50 nm. On the other hand, to produce an NAD^+ dependent

biosensor – as reported by *Mie et al.* [26] – a 3 mm gold wire is immersed in 35mM HCl. By applying a constant potential of 1.21 V for 2-30 minutes, an NPG with an Rf of 1.4-10 and a pore size of 20-40 nm is formed. Finally, to obtain a dopamine sensor – as in *Saénz et al.* work [18] - a 25 µm gold wire was immersed in 0.5M H_2SO_4 with Ag/AgCl as CE and RE. By applying a constant voltage of 2 V for 20 minutes, the team obtained an R_f of 143 and a pore size of 30-50 nm. For this last application, there is a need to record a reverse scan to reduce the surface.

Table 1 - Summary of the applications and the respective reaction parameters used in each research.

	Glucose [18]	*NAD^+ dependent* [17]	*Dopamine sensor* [19]
Electrolyte	1M KCl	35mM HCl	0.5M H_2SO_4
WE diameter	2 mm	3 mm	25 µm
Counter electrode (CE)	Pt wire		Ag/AgCl
Reference electrode	Ag/AgCl		
Applied potential [V]	1.37	1.21	2
Reaction time	400 sec	2-30 min	20 min
Pore size [nm]	50	20-40	30-50
Roughness factor (R_f)	750	1.4-10	143

1.3. Glucose sensing

Glucose sensing using electrochemical methods has gained significant attention due to its importance in various applications, such as medical diagnostics of different diseases [51] and diabetes management [3]. However, the oxidation of glucose at Au electrodes typically requires high potentials, which can lead to potential interference from other biological molecules (e.g., ascorbic acid). To address this issue, extensive efforts have been devoted to minimizing interference and enhancing the selectivity of electrochemical sensors.

One approach is the modification of electrode surfaces to mitigate interference from foreign substances and improve the sensor response [29]. Also – as reported by *Lamy et al.* – the morphology and crystallographic orientations of gold electrodes play a critical role in determining their electrocatalytic activity and selectivity [30]. Among the different gold planes, according to *Napporn et al.*, the Au (100) has been shown to be more active than (111) and (110), proving the influence of this parameter in glucose sensing [31].

As this happens, researchers have been exploring the use of nanomaterials and surface modifications to overcome these challenges in electrochemical glucose oxidation and sensing, and recent studies have focused on addressing these issues for various analytes, including NAD^+, dopamine, and acetaminophen [29].

Gold has been considered a great metal for glucose oxidation since it holds unique advantages due to its more negative oxidation potential in neutral and alkaline media compared to other metals [30]. Consequently, gold electrodes have been extensively studied for amperometric glucose-sensing applications. The utilization of nanostructured Au has shown promising results, exhibiting high electrocatalytic activity towards glucose oxidation, which is notably absent in flat Au surfaces [29]. Therefore, the structure sensitivity of glucose oxidation on gold electrodes has attracted recent attention [30], emphasizing the need for a comprehensive understanding of the electrode surface's crystallographic orientation to optimize glucose sensing capabilities.

In this project, the main goal will be developing an efficient and easy anodization technique to create nanostructures which will lately be applied in electrochemical biosensors for glucose sensing. Besides, the versatility of the technique will be tested by nanostructuring gold microelectrodes to apply in impedance biosensors.

2

MATERIALS AND METHODS

1.1 Preparation of gold electrodes

The Au film samples used in these experiments were obtained by *RF Magnetron Sputtering*. Applying a power deposition of 80W, a 700 nm Au layer was deposited on top of a borosilicate glass wafer with a titanium layer, used to enhance the adhesion of glass-gold. The pressures applied were 1×10^{-2} mbar as the working pressure and, 4×10^{-5} mbar as the base pressure. Then, to decrease the impurity contamination, a positive *S1818* photoresist layer is deposited on top of the samples. Finally, the wafer is diced into 7x14 mm samples using a jet water mechanism.

Afterwards, the prepared samples are immersed in acetone for 5 minutes to remove impurities from the electrode and also to strip the photoresist layer. Finally, the samples are rinsed with the same solvent, then, IPA, deionized water (DI), and carefully dried with N_2 gas.

To ensure a fixed exposed area to the electrolyte a strip of tape is placed on the samples. For this stage, an electrode aligner was used (**Appendix A** - Figure A6), where a piece of tape should adhere to the sample along the red strips schematized. Using this handmade device, the sample should be aligned and prepared to guarantee a 7x7 mm active area.

1.2 Preparation of the solutions

To proceed with the cleaning protocol a 500 mL solution of 0.5M of sulfuric acid *(7664-93-9)* (H_2SO_4 ≥ 96%) was prepared by adding 14.0 mL of the solution to 486 mL of DI. Then, for the anodization, different potassium chloride (KCl ≥ 99.9%) solutions were prepared: 0.3M, 0.5M, and 0.7M. For this, it was necessary to dissolve 11.18 g, 18.63 g, and 26.09 g of KCl *(7447-40-7)* in 500 mL of DI water. All the chemicals mentioned were obtained from *Sigma-Aldrich (Germany)* and were used without further purification.

1.3 Cleaning protocol

A cleaning electrode protocol was implemented during this project to avoid any type of contamination which could affect the anodization itself.

Firstly, the triple junction provided by *Sigma-Aldrich (Germany)*, used as an RE in this project should be prepared. For this, the 3.8M KCl solution inside the bridge should be replaced by 0.5M H_2SO_4 to avoid chloride leakage. Since this leakage can compromise the final results, the inside and outside of the reference need to be carefully rinsed with DI water to avoid any remaining chloride ions.

The prepared RE was then immersed in a beaker containing 0.5M H_2SO_4. For ease of setup, the platinum wire used as a CE was attached to the RE. Finally, the gold sample was placed in a clip and immersed in the electrolyte solution, making sure the connection region was completely dry and the WE was parallel to the RE.

As schematized in Figure 3, is important to guarantee the electrodes are in the following order, WE – CE – RE. It is essential to maintain the WE near the CE to minimize the RE effect explained in the last chapter.

The electrodes were connected to the potentiostat *Gamry Ref 600+* (Figure 3), and a 30-cycle-cyclic voltammogram was recorded considering the potentials between -0.2 V and 1.6 V, at a scan rate of 100 mV/s and a step size of 10 mV, Table A1. Besides being a source of cleaning, this cyclic voltammogram was also a means of characterization and activation of the electroactive area.

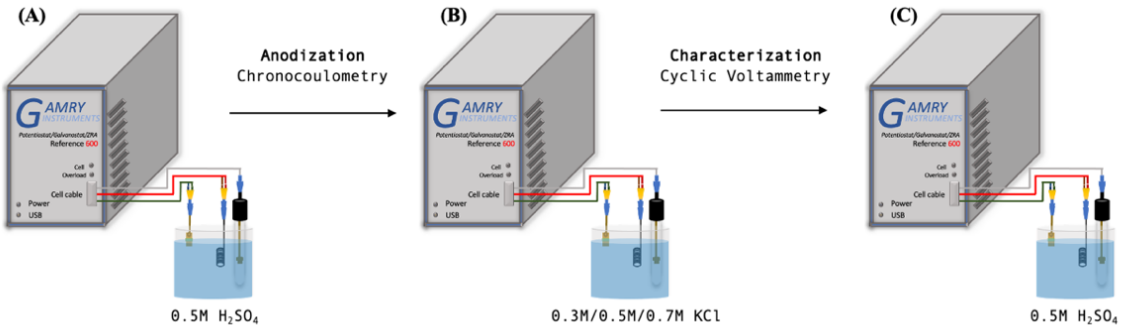

Figure 3 - Schematic of the set-up used for the fabrication of nanoporous gold. (A) Cleaning and activation of the electrodes by CV, (B) Anodization by chronocoulometry, and (C) Characterization of the samples by cyclic voltammetry.

1.4 Set-up optimization

To create a fixed and stable setup, as required for CV measurements, a protocol was developed. This protocol involved: i) the use of a positive photoresist *S1818* PR spin-coated at 3000 rpm for 45 min to protect and define the 600 nm of Au electrode deposited by sputtering on top a borosilicate glass with a Ti layer; ii) the use of a bridge reference electrode Ag/AgCl filled with 0.5M H_2SO_4 to avoid leakage of the chloride ions to the electrolyte; iii) the correct positioning of the electrodes by ensuring a parallel position of the WE in respect to the RE and iv) the definition of a constant/fixed exposed area using an alignment rod and obtaining a exposed area of 7x7 mm. Further details on this optimization can be found in **Appendix A.**

2. Anodization Process

The cleaned sample was rinsed with DI water and dried with N_2 gas. Then, the sample along with the Ag/AgCl RE and the CE, was immersed in the same electrolyte with different concentrations 0.3M, 0.5M, and 0.7M KCl, to understand the influence of chloride concentration in anodization.

Afterwards, the electrodes were once again connected to the potentiostat to record chronocoulometry. The current generated was integrated making it possible to monitor the variation of charge with time. For this project, 1.5 V was defined as the optimal potential, and the charges tested were: 200, 400, and 600 mC.

3. Area measurements

For these measurements, the sample was cycled 30 times in 0.5M H_2SO_4, scanning a potential from -0.2 V to +1.6 V vs. Ag/AgCl/ H_2SO_4 sat.

To obtain the value of the electroactive surface area, the reduction peak of the CVs was monitored before and after anodization. The integration of the reduction peak gives the charge generated in the redox reactions and allows the determination of the real electrode area that is obtained using the following equation:

$$\mathrm{ESA} = \frac{Q_0}{v \cdot Q_{os}}, \qquad [3]$$

where Q_0 represents the area under the reduction peak (mA·V), obtained by integrating the area in the software *Echem Analyst.*, v is the scan rate defined for the CVs (V/s), and Q_{os} is the charge per surface area for a gold oxide layer, which is equivalent to 384 C/m^2.

4. Glucose sensing

The PBS solution was prepared by dissolving 15.5 g of heptahydrate ($Na_2HPO_4 \cdot 7H_2O > 98.0\%$) and 5.8 g of sodium phosphate monobasic ($Na_2HPO_4 > 98.0\%$) in 1 L of DI. Another solution was prepared by adding 5.6 g of potassium hydroxide *(1310-58-3)* (KOH, 86.2%) to 25 mL of DI. The KOH solution was carefully added to PBS to increase its pH to 7.4.

Using the formulated PBS solution, glucose mixtures were prepared with different concentrations, such as 0.5, 1, 2, 4, 8, and 10 mM. For this 0.27 g of D-glucose *(50-99-7) (*$C_6H_{12}O_6 > 99.5\%$) is added to 15 mL of PBS, resulting in the 10mM glucose solution. The following concentrations were prepared by means of dilution. All the chemicals used for these experiments were obtained at *Sigma-Aldrich (Germany)*, with the exception of KOH which was purchased at *VWR Chemicals (USA)*.

To do these tests, a platinum wire (*CE*), a bridge of the RE filled with PBS, and a gold electrode sample (*WE*) were immersed in bare PBS cycling 30 times a potential between - 0.2 V and + 1.2 V vs. Ag/AgCl/PBS sat., using a multi-channel potentiostat (*MultiPalmSens4, PalmSens, Netherlands*). These first cycles assisted the activation of the surface area for glucose sensing. After this, three cycles were recorded for each concentration to obtain the calibration curves.

5. Morphological and structural characterization of the electrodes

To analyze and study the different structures, after and before anodization, Scanning Electron Microscopy (SEM) images were taken using a *PHILIPS* scanning electron microscope *XL30 FEG*. The structural characterization was performed using X-ray Dffraction (XRD) using a *PANalytical's X'Pert PRO* diffractometer.

6. Microelectrodes preparation

To prove the anodization technique is also capable of roughening microelectrodes to apply in an impedance sensor to trap single cells, a side project was developed. This not only showcases the technique's versatility by effectively roughening both gold electrodes and microelectrodes but also highlights how adjusting specific reaction parameters can generate various structures suitable for a wide range of applications.

For this, the sample's fabrication used in this project can be summarized as: i) Deposition by sputtering of 200 nm Au with a Ti adhesion layer on a glass wafer; ii) Lift-off processes to pattern the gold electrodes; iii) Spin-coating of SU8 layer on top to pattern and define the electrodes.

Then, for cleaning purposes, the sample was immersed in acetone for 3 minutes to remove the photoresist layer on top. Afterwards, it was rinsed with the same solvent, IPA *(67-63-0)*, and the microelectrodes were set aside for drying. Afterwards, the sample was inserted in a holder and a PCB was placed on top. To calibrate the microelectrodes an impedance analyzer (*Wayne Kerr 6500B*) was used. For this step, to ensure the connections, the system was closed with screws.

In order to measure the microelectrodes impedance, a silicon tube was cut with the same height as the PCB and filled with 1:100 PBS. Then, to proceed with the anodization, the PCB was connected to the function generator and the desired voltage (V_{PP}) was applied with a pulse width of 1 second, a period of 10 seconds, an offset voltage of 0 V, and an edge time of 5 nanoseconds.

Finally, the signal was generated for one second, the bubbles formed were removed and the impedance was measured again to compare the data before and after anodization.

3

RESULTS AND DISCUSSION

As described in the previous chapter, firstly the gold was deposited on top of a borosilicate glass wafer along with a Ti layer working as an adhesion layer. After obtaining the gold wafer, it was diced into 7x14 mm samples with a jet water mechanism. Then, the area of the sample was restricted to 7x7 mm recurring to the electrode aligner shown in **Appendix A** (Figure A6).

Prior to the preparation of the samples, they went through a cleaning and anodization protocol which were optimized for this project. As can be seen in Figure 4, the colour of the sample changed from yellow to orange after anodization, indicating the creation of structures on the electrode surface. It is clear that not all the samples were affected in the same way. This proved the influence of certain reaction parameters in the structuring of the surface, such as electrolyte concentration and imposed charge. The samples represented in Figure 4 were produced at different electrolyte concentrations and imposed charges.

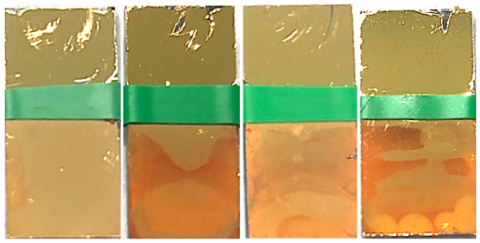

Figure 4 - Picture of the samples (7x14 mm) structured by anodization in a chloride medium.

To compare the behaviour and the area of the electrode before and after anodization, cyclic voltammetry (CV) experiments were conducted. This electrochemical technique is based on scanning a certain potential range during several cycles using a potentiostat to apply the potential, measure the signal produced in the reaction, and generate the CV. As this happens, it is considered an excellent approach to obtain valuable information and characterize the samples [32]. It also provides insights into redox potentials, reaction mechanisms, kinetics of electrochemical processes, and detection of electroactive species [35, 36].

In the first region, the current is associated with the charging of a double-layer capacitance (C), expressed as $j = C(dE/dt)$, where j is the current. In the second and third regions, surface redox reactions occur, leading to a faradaic current flowing through the interface [32].

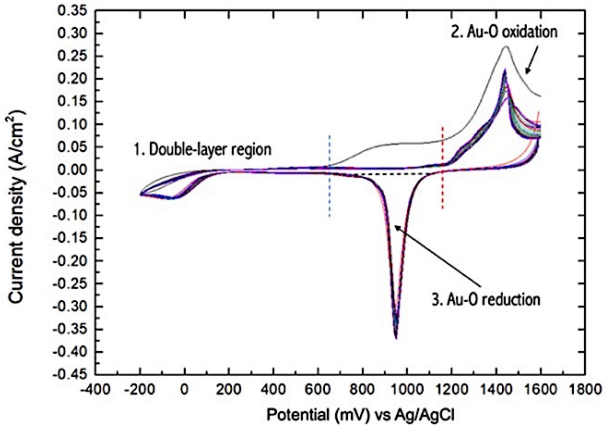

Figure 5 - CV profile recorded in 0.5M H_2SO_4 with an Ag/AgCl as RE and Pt wire as CE.

As represented in Figure 5, the signal obtained gives information about the reactions present in the electrolyte, the formed oxide gold planes and also, the value of the actual electrochemical surface area of the electrode. For this reason, to monitor the effects of the roughening in the gold electrode, the CV should be recorded twice, before and after the anodization.

Even though this method is widely used, it has some limitations. Its measurement's reliability and accuracy depend on factors like scan rate and cleanliness of the interface (electrolyte/electrode). Besides this, the chemical and physical state of the Au surface significantly influences the outcomes. To avoid deviations in results, care must be taken to ensure the cleanliness of solvents, chemicals, glassware, and tweezers [32][33].

1.1. Optimization of the cleaning protocol

One of the most important steps for this project is the electrode cleaning protocol. The protocol consisted of immersing the sample, a platinum wire (CE) and an Ag/AgCl RE in 0.5M H_2SO_4. To obtain the signal, a CV was recorded by scanning 30 times the potential range between - 0.2 V and + 1.6 V at a scan rate of 100 mV/s.

By taking into account the parameters discussed in **Appendix A**, the signal generated showed an improvement when compared to the first measurement. In this chapter, all the potentials mentioned are referred to Ag/AgCl/H_2SO_4 sat., the RE used. To assess the electrochemical behaviour of the electrodes, CV experiments were performed on pristine samples and optimized samples. The CVs are shown in Figure 6.

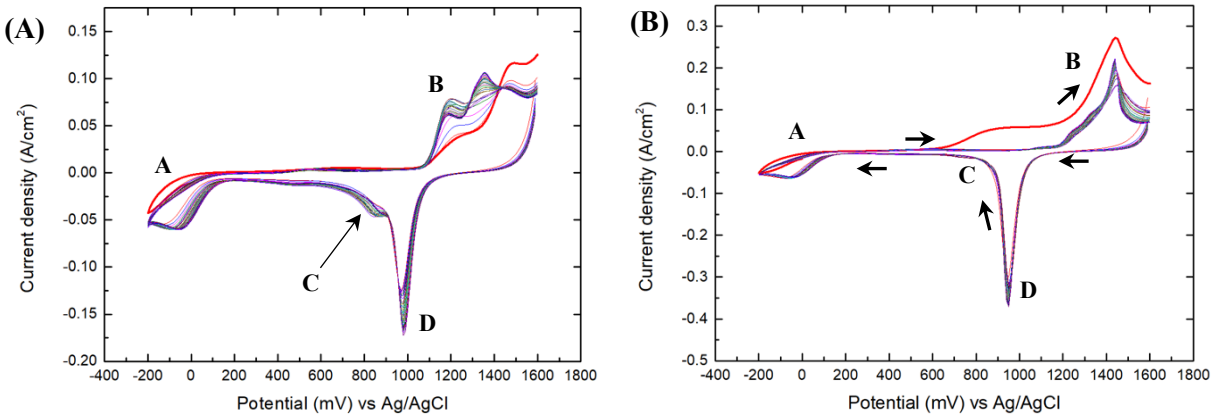

Figure 6 – CVs obtained in 0.5M H_2SO_4, (A) before and (B) after the corrections in the protocol, at a scan rate of 100 mV/s and a step size of 10 mV.

When comparing both CVs (Figure 6), it becomes evident that the first one displays a notably less stable signal in contrast to the plot (B). In the CVs shown, several regions are identified (A to D) where the comparison between both curves can be discussed. The instabilities are attributable to several factors, mainly evident in the changes in double-layer capacitance (**region A**), and the oxidation reaction (**region B**). As described in **Appendix A**, some cautions need to be taken into account, being one of them the photoresist (PR) layer. This additional layer impacted the signal, turning region A more stable when compared to the CVs prior to and post-application of the PR. This dissimilarity in the behavior comes from the presence of impurities on the electrode surface which were removed by the deposition of a PR layer on top of the electrode. This one showed to be capable of protecting the surface Au from damage and external contamination.

A different reason for the instability observed during the experiments which affects regions A and B pertains to the condition of the contact area. The contact area of the WE was responsible for facilitating the connection between the potentiostat and the said electrode. This one stands as the site wherein the reactions of interest occur, specifically, the reduction and oxidation of gold represented in the CV. Any potential

irregularities with the connections might compromise the signal measured. For this reason, it was important to guarantee the contact area was completely dry and free of scratches.

An additional phenomenon was identified in **region C**, denoted as chloride (Cl^-) leakage, and represented by an extra peak at 0.8 V [39]. In Figure 6 (B), on the optimized sample, this peak disappeared due to the usage of a bridge on the RE. This absence serves to substantiate that the bridge plays a huge impact in the signal measured, the replacement of 3.8M KCl with 0.5M H_2SO_4 inside of the RE successfully vanished the Cl^- effects. Apart from this, it was also seen that the second cathodic peak (0.8 V) demonstrates an increase in magnitude proportionally to Cl^- concentration. This phenomenon can be attributed to the process of electrodeposition of Au from $AuCl_4^-$ species [39].

The **region D** which corresponds to the reduction peak, provides evidence that the redox reaction occurs at a different potential prior to - 990 mV - and after - 920 mV - the optimization of the protocol. It was of supreme importance that the redox reactions happening between the WE and the electrolyte occur under uniform conditions. The observed shift in the signal can be attributed to the electrode position which should follow the sequence – WE, CE, and RE. To avoid this factor influencing the electrochemical potential, measures have been implemented to guarantee consistent electrode alignment throughout both the anodization process and the cleaning protocol. To this end, a custom-designed cap, explained in **Appendix A** (Figure A6), has solved this problem. Its efficacy is evidenced by the consistency in the reduction potential across all measurements, happening at around 920 mV.

With the insight taken from the optimization of the cleaning protocol, it was possible to designate the Cl^- leakage as the most impactful factor at this stage. This comes from the misleading results this phenomenon leads to since the calculation and the monitorization of the electrochemically active area have been compromised since the beginning. However, all the other parameters can't be despised.

Finally, as evidenced in the CV presented below, after the optimization of the set-up, the recorded signal from three different samples shows a similar current magnitude generated in the reduction reaction. This is of vital importance since, as previously demonstrated, the area of the reduction peak affords the means to obtain the real surface area of the electrode.

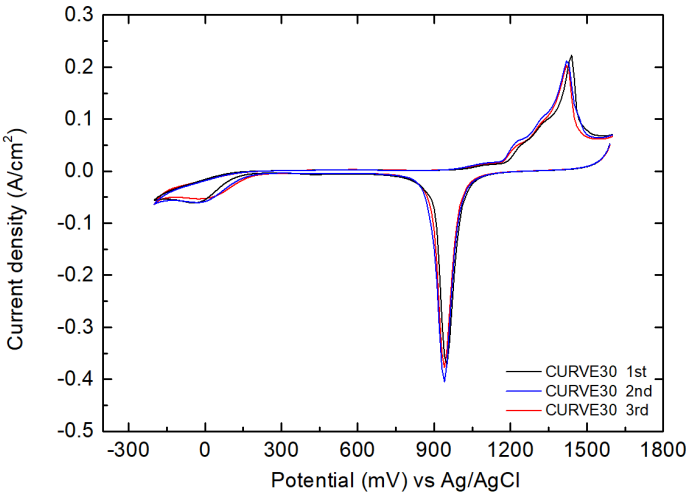

Figure 7 - CV of bare gold, obtained in 0.5M H_2SO_4 at a scan rate of 100 mV/s and a step size of 10 mV. CV corresponded for three different samples.

The CV present in Figure 7, shows that the three samples exhibit an identical reduction peak meaning they present equivalent surface areas. The outcomes from the analysis done for this project demonstrate an average initial area of 0.72 $cm^2 \pm 0.06$. The standard deviation reflects the short difference in the initial area of all 75 samples tested, which serves as evidence to validate the efficacy of the electrode aligner in producing

electrodes with similar areas of 7×7 cm. Beyond this, the data also corroborates the effectiveness of the cautions employed and the successful realization of the optimization of the cleaning protocol.

1.2. Anodization of the Electrodes

As can be seen by the samples represented in Figure 4, the result of the anodization was different with the variation of certain parameters, showing their impact on the final outcome of the anodization itself. Several factors can influence the performance of the anodization process. It includes the electrolyte type and concentration, Cl^- concentration, pH, scan rate, reaction time, and the nature of the applied potential whether in a scanned or constant mode. Due to the time limit of this project, the optimization of all these parameters was unfeasible to undertake. Nevertheless, a partial analysis was done wherein the optimal potential was defined and distinct electrolyte concentrations were tested with the intent of understanding the impact of this particular parameter in the final outcome. Besides, for each concentration, the samples were submitted to three different charges. As in the previous subsection, all the potentials mentioned are referred to $Ag/AgCl/H_2SO_4$ sat., the RE used.

1.2.1. Anodization by cyclic voltammetry experiments

By the findings [40-43], the CV obtained in Cl^- solutions, in this case, 0.1M KCl can be divided into two main domains. The initial domain, designated as **region A**, is indicative of Au electrodissolution and corresponds to the anodic current. The second one is characterized by a cathodic peak, **region B**, which is related to the electrodeposition of the dissolved metal.

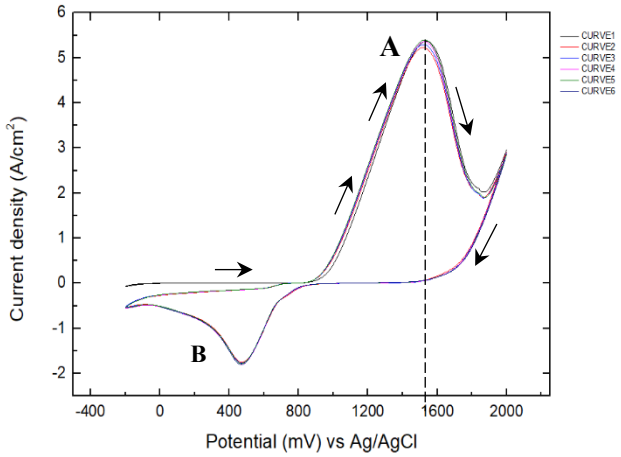

Figure 8 - CV recorded in 0.1M KCl at a scan rate of 100 mV/s and a step size of 10 mV.

At first, within the potential range of 300 mV to 1100 mV, it starts the process of Au electrodeposition followed by the diffusion of Cl^- ions onto the gold surface at potentials between 1200 mV and 1400 mV [38] [39]. Further, at voltages around 1550 mV, a phenomenon of Au passivation occurs which is attributed to the formation of an oxide layer on the surface of the Au electrode. Upon reversing the scan direction, at potentials of 460 mV the surface oxide is reduced due to the reduction of the complexes of $AuCl_2^-$ and $AuCl_4^-$ [40].

Upon gaining insights into the anodic behaviour of Au, the optimal applied potential for this project was determined as 1.5 V vs. Ag/AgCl/KCl sat.. This value was selected due to its proximity to the point just before Au passivation, a parameter acknowledged in the literature to be beneficial for effective anodization.

Furthermore, given that anodization involves the transformation of Au into its oxide form, the selection of 1.5 V aligns with the occurrence of oxide layer formation on the Au surface, being considered the best option for the roughening technique.

In order to test the influence of the reaction time, three identical samples were submitted to chroamperometric experiments at 1.5 V for 60 s, 120 s, and 180 s. The same samples were analyzed by CV experiments to compare the initial with the anodized state. The CVs for bare gold (black line) and one of the anodized samples for each condition are presented in Figure 9.

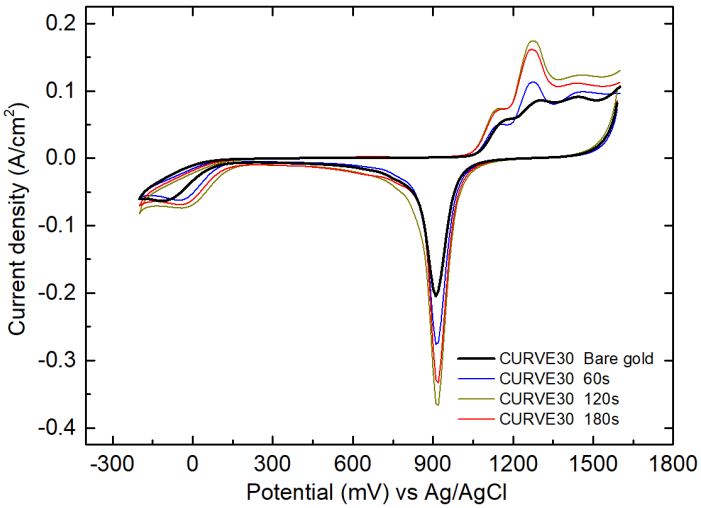

Figure 9 - CVs obtained in 0.5M H_2SO_4 at a scan rate of 100 mV/s. Results obtained before (bare gold) and after anodization. The anodization was done by chronoamperometry for different reaction times (60 s, 120 s, and 180 s).

To initiate the anodization process while maintaining a constant voltage of 1.5 V, chronoamperometry was employed on three samples in a 0.1M KCl solution for cycles of 0.01 seconds. A platinum wire served as the CE, and an Ag/AgCl/KCl sat. electrode was employed as the RE. To assess the influence of reaction time, the anodization was executed over periods of 60 s, 120 s, and 180 s.

Upon comparing the reduction peak before and after anodization, it was clear that the electrode's surface had been roughened. By following chronoamperometry, it was possible to roughen the gold electrodes, since it could enhance the current by 20%.

Even though there was a clear change in the area post-anodization, the goal was to achieve a greater roughening of the electrode. For that, chronocoulometry was tested as a different approach.

This technique is valuable for anodization on Au electrodes due to its ability to precisely measure the total charge passed during the process, enabling quantitative assessment and understanding of electron involvement. This is crucial given gold's common use in electrochemical studies due to its conductivity and stability. It helps assess charge efficiency, revealing how effectively anodization occurs. Additionally, chronocoulometry provides control by allowing the application of a constant potential for a defined charge, aiding in the study of anodization kinetics and experimental optimization [34].

In light of these considerations, a series of tests were conducted utilizing chronocoulometry to examine the impact of electrolyte concentration and applied charge on the Au electrode. The selected concentrations were 0.3M, 0.5M, and 0.7M KCl, while the designated charges were 200 mC, 400 mC, and 600 mC. To ensure the technique's reproducibility, each condition was executed on three separate samples, as depicted in the results presented in **Appendix B** (Figure A10).

At first, lower concentrations were considered, such as 0.1M KCl, however, this yielded minimal variation in the area, below 10% difference, and for the lowest charge, the experimental duration exceeded an hour. Since one of the project's emphases was on developing a facile and rapid technique to generate NPG, this concentration was excluded and replaced with 0.3M KCl, which exhibited more promising outcomes.

Regarding the chosen charges, they were initially defined by the charges generated in the choroamperometry trials, which were approximately 40 mC and 60 mC. However, the preliminary outcomes for these charges demonstrated negligible differences in the area. Hence, the ultimate charge values were set higher to yield more discernible effects.

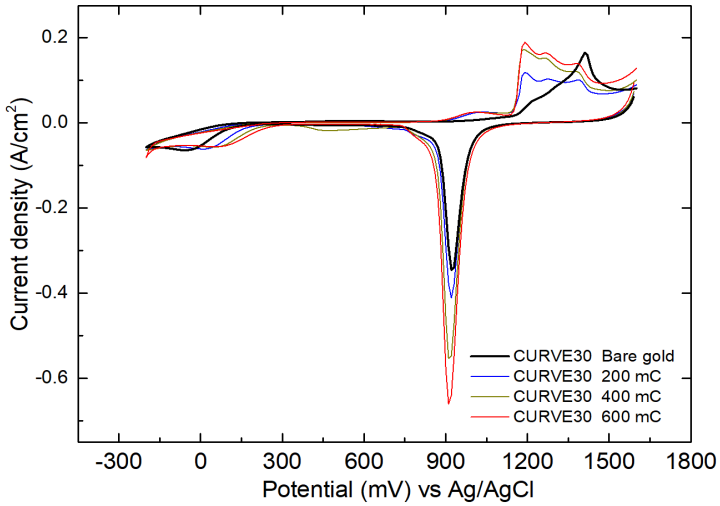

Figure 10 - CVs recorded in 0.5M H2SO4, at a scan rate of 100 mV/s and a step size of 10 mV. Signals correspond to one sample per condition. NPG was prepared by chronocoulometry in 0.3M KCl where the applied charge was: (blue) 200 mC, (dark blue) 400 mC, and (red) 600 mC.

The outcomes shown in Figure 10 delineate the behaviour of the Au electrode after the anodization, following chronocoulometry in 0.3M KCl solution. The CVs for each condition reflect similar results for the three samples, as evidenced by the low standard deviation of the electroactive area measured - Figure A8 - 0.09 cm^2 for 200 mC, 0.02 cm^2 for 400 mC, and 0.1 cm^2 for 600 mC. By comparing the results before and after anodization, Figure 10, was observable a maximum enhancement of 24.40% (600 mC) in the area of the gold electrode.

When comparing the CVs prior to anodization (black line – Figure 10) and post, there was noticeable a difference in the oxidation region. In consonance with the literature [19], the oxidation section serves as an indicator of the presence of Au oxides in the sample.

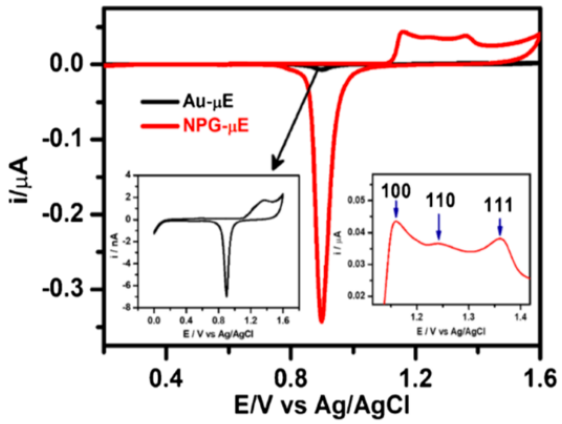

Figure 11 - CVs of bare Au-μE and NPG- μE in 0.5M H_2SO_4 solution. Scan rate: 0.1V [19] Anodization recorded on 0.1M KCl.

As schematized in Figure 11, the first oxidation peak at around 1.15 V vs. Ag/AgCl represents the orientational plane (100), while 1.25 V corresponds to Au (110), and 1.35 V to Au (111). Comparing the signal from the literature (Figure 11) with the CVs obtained in this project (Figure 10) it was clear the presence of

three oxidation peaks at around the same voltages, which indicates the Au crystallographic planes present in the new electrode's surface.

Before any surface treatment, Figure 7, the dominant gold plane was Au (111) at an anodic potential of nearly 1.45 V. However, after anodization, there is an evident shift to Au (100) at a potential around 1.25 V. This can be ascribed to the reconstruction process of the gold surface during anodization, which engenders distinct preferences for the grown crystal facets. This structural reconstruction comes from the Au dissolution induced by chloride, resulting in the reorganization of the deposited Au into a more stable orientation [19]. Consequently, it was deducible that bare Au (before anodization) and NPG (after anodization) have different facet contributions, which can influence the behaviour of the electrode, as will be explored in this chapter. Moreover, the presented results prove that this simple, user-friendly, and rapid anodization procedure possesses the capacity to alter the atomic structure of the gold surface.

Still regarding the oxidation region, there are discernable differences between samples submitted to charges of 200 mC and 400 mC (Figure A8). The difference noticed can potentially appear from some solution or sample contamination, which in turn might impact the mechanism of Au electrodissolution, however, there is a need for further study in this area. As already explained, electrochemistry reactions exhibit pronounced sensitivity, and the execution of these tests involved the use of four different electrodes (Pt wire, Ag/AgCl/KCl sat., Ag/AgCl/H_2SO_4 sat., and gold sample), and two different solutions (0.5M H_2SO_4 and 0.3M KCl) meaning there was a great margin for contamination. One measure to mitigate this contamination, besides cleaning everything carefully, involves conducting these experiments in a clean room, where the impurity level should be significantly less than in a conventional laboratory.

Lastly, it was evident that the optimal outcomes were obtained through the application of a 600 mC charge in a solution of 0.3M KCl. The results are aligned with the expectations, as a higher charge imposed on the sample increases the gold electrodissolution, thereby provoking a more pronounced electrode roughening.

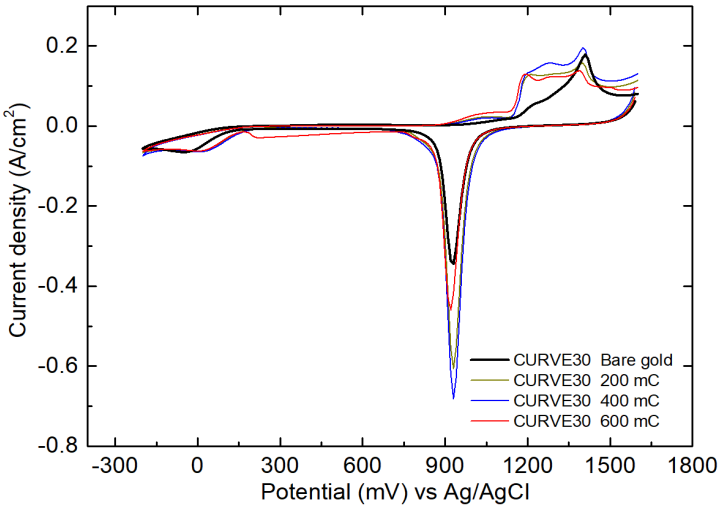

Figure 12 - CVs recorded in 0.5M H_2SO_4, at a scan rate of 100 mV/s and a step size of 10 mV. Signals correspond to the three samples for each condition. NPG was prepared by chronocoulometry in 0.5M KCl where the applied charge was: (light blue) 200 mC, (dark blue) 400 mC, (red) 600 mC.

The results derived from the experiments conducted in 0.5M KCl exhibited a great level of reproducibility, with the exception of one sample obtained at 600 mC (Figure A9). The standard deviations were – Figure A8 – 0.05 cm^2 for 200 mC, 0.1 cm^2 for 400 mC, and 0.3 cm^2 for 600 mC. In terms of comparison, the results indicated that the application of the lowest charge yielded an area enhancement of nearly 54.2%, the 400 mC had a maximum of nearly 80%, while the higher charge resulted in an increase of around 18% with an outlier sample which enhanced the area in 72.3%.

Regarding the formation of gold planes, a majority of the samples presented a preferential growth for the facets Au (111) and Au (100). As can be compared, the oxidations peaks represented in Figures 11 and 12, the preference for the crystallographic planes changed with the electrolyte concentration. As previously reported, performing the anodization in higher Cl^- content can alter the facet contributions of Au. At the initial stages, the dissolution of Au occurs at a more accelerated pace, leading to variations in the Au reorganization and consequently resulting in the formation of different planes.

It is worth noting that the CV of the samples obtained using 0.5M KCl at 400 mC exhibited a higher degree of stability and reproducibility and at the same time a higher roughening of the electrodes. In contrast, for 0.5M KCl, 600 mC presented the worst results. This disparity can be attributed to the fact that 600 mC might be excessive for a concentration of 0.5 KCl. Under this condition, the Au electrodissolution might have reached its limit, meaning that a furthered roughening of the gold electrodes cannot be achievable. This highlights the notion that an excessive charge might not be the best solution for all the concentrations tested.

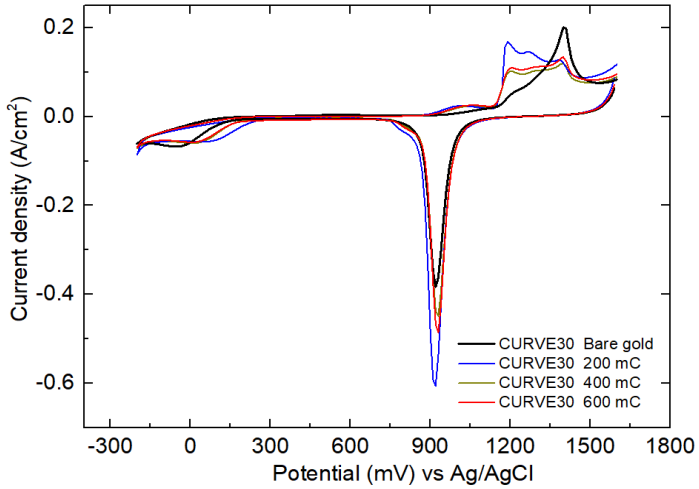

Figure 13 - CVs recorded in 0.5M H_2SO_4, at a scan rate of 100 mV/s and a step size of 10 mV. Signals correspond to the three samples for each condition. NPG was prepared by chronocoulometry in 0.7M KCl where the applied charge was: (light blue) 200 mC, (dark blue) 400 mC, and (red) 600 mC.

The outcomes presented in Figure 13 illustrate the behaviour of the Au electrode after anodization performed by chronocoulometry in 0.7M KCl. It was evident that the CVs of the three samples, for each condition, have shown congruent results, with the exception of 600 mC (Figure A10). These sets of samples presented a standard deviation of - Figure A9 - 0.1 cm^2 for 200 mC, 0.05 cm^2 for 400 mC, and 0.2 cm^2 for 600 mC. By comparing the results before and after anodization, it was perceptible a maximum enhancement of 50.8% in the gold electrode's area.

Among all the samples analyzed, the results produced in 0.7M KCl exhibited greater dissimilarities in the Au planes formed, with the exception of 200 mC (Figure A10 (A)). This phenomenon might be attributed to the high Cl^-concentration of 0.7M, which can be excessive for anodizing the electrodes. Instead of creating an oxide layer on top of the sample, the Au is being etched away. As expected, this effect became more pronounced with higher applied charges, which can be proved not only from the CVs but also from the colour of the samples after the anodization (grey). For this reason, the lowest charge implied was the optimal approach to employ, since it was less aggressive for this concentration. Additionally, this choice serves to minimize the reaction time, in other words, it limits the exposure of the Au surface to the Cl^-solution avoiding the etching of the metal.

From the analysis of the CVs, assessing all the charges and concentrations, the most favourable outcomes emerged from the samples produced in 0.5M KCl, applying a charge of 400 mC. Besides all the reasons explained, the three samples displayed good reproducibility and roughening of the gold electrodes.

This condition aligns with the project objectives: roughening in just 15 seconds with a user-friendly, rapid, simple, and costless technique.

1.3. Colour change

In addition to the changes in the electrochemical behaviour of the sample registered by the CVs, it was also observed a variation in the colour of the samples. A predominant outcome of the majority of the prepared samples was the transition from a yellow colour (bare gold) to an orange shade (anodized gold) – Figure 14. This characteristic might indicate the presence of trivalent gold oxide (Au^{3+}) in the formed film, which was reduced in anodization causing the change of colour [41].

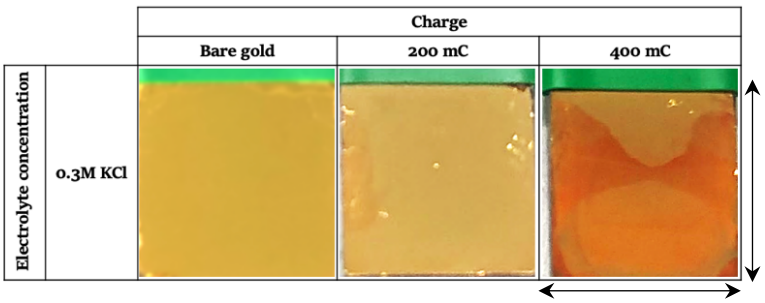

Figure 14 -Electrode's colour change before anodization (Bare gold) and after anodization in 0.3M KCl for the different charges imposed (200 mC and 400 mC) (Scale: 7×7 cm)

The images of the samples reveal a non-uniformity in the anodization, in other words, the change of colour was not constant along the surface. This could be attributed to oscillations in the anodic current. According to *Podestá et al*., solutions containing chloride generate a passivity current dependent on stirring conditions. In unstirred solutions, these periodic current oscillations only appear when the chloride concentration exceeds a certain threshold. As reported, each period involves a large drop of the anodic current which is called the active region and a lapse of relatively low current known as the passivation region. This current fluctuation has been attributed to the presence of soluble Au species in the initial solution [41].

Besides this, *Podestá et al.* also noticed that the morphology of the anodized substrate changed according to the solution composition. In scenarios where the electrolyte remains unstirred, the anodization process may lead to the development of an uneven oxide layer, thus yielding a non-uniform outcome in terms of surface alteration.

As this happens, an option to create a uniform Au oxide layer is performing the anodization on stirring conditions [41], which will uniformize the electrolyte solution, and consequently, the ions participating in the redox reactions happening in the interface. Another possibility is using a platinum mesh CE instead of a wire. This strategic substitution offers the advantage of augmenting the available surface area for reactions, meaning an increase and uniformity of the electric field generated.

1.4. Scanning Electron Microscopy (SEM)

SEM images in Figure 15 show the NPG surface and bare Au with magnifications of 5000x and 10000x. By this analysis, it was clear that the surface of the Au electrode suffered changes with the anodization having a noticeable higher grain size. Since this happens, it was possible to affirm that anodization in 0.5M KCl done by chronocoloumetry could roughen the surface of the electrode.

This consideration served to conclude that indeed a nanostructure was created on top of the Au surface, and it was responsible for the differences noticed in the colour of the electrode and the glucose sensing.

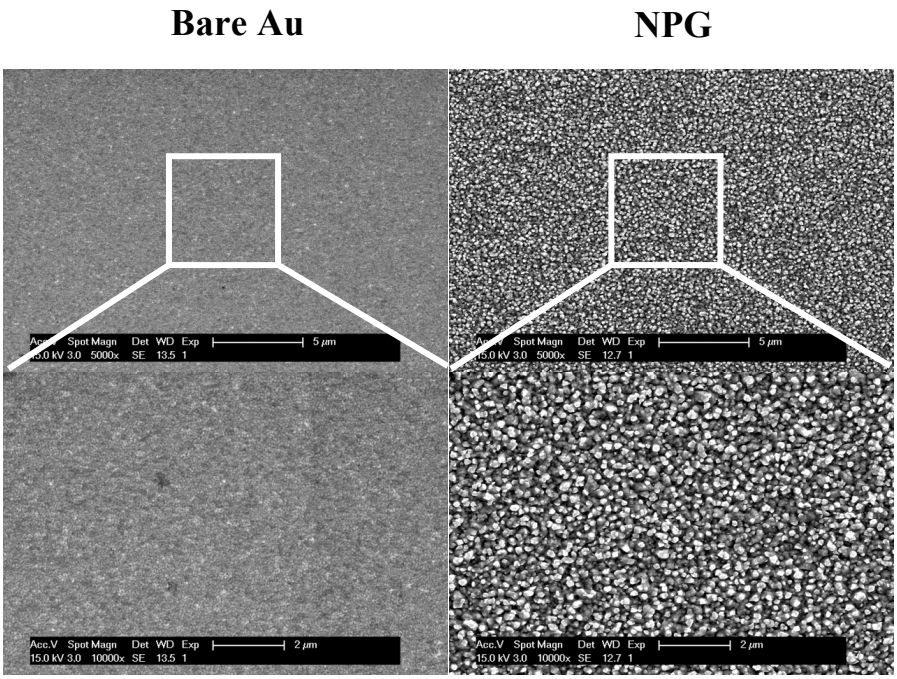

Figure 15 - SEM images of the Au electrodes before and after anodization (0.5M KCl 400 mC). First column it is the bare Au and in the second NPG. The first line corresponds to a magnification of 5000x and the second to 10000x.

1.5. X-Ray Diffraction Analysis

As previously discussed, it was believed that the crystallographic orientation of the metal, Au, had an impact on both, chloride resistance and glucose oxidation sensitivity.

From what is known up to now, a higher amount of Au (111) might be related to higher resistance to chloride poisoning and, at the same time, a greater sensitivity.

An XRD to both, bare and nanostructured samples, was performed. As shown in Figure 16, bare gold presented the crystallographic planes (111), (200), (220), and (311). Even though the anodized electrodes presented the same planes, their magnitude changed from prior to post-anodization. The NPG contains a greater preferential growth of Au (220) and less of Au (111).

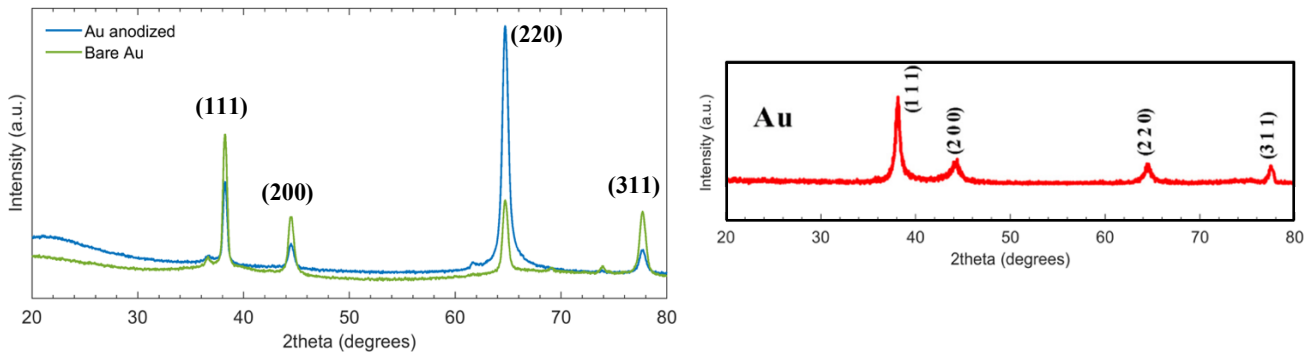

Figure 16 – (right) XRD analysis of the bare and anodized samples (0.5M 400mC). (left) Au peaks XRD from literature.

By adding this result, to the ones elucidated in the next sub-chapters - CV, chronoamperometry, and chloride poisoning - is evident the impact of crystallographic planes in the glucose electrooxidation and poisoning. The reduction of Au (111) content leads to the conclusion that this specific plane plays a pivotal role in glucose adsorption onto the electrode surface, related to sensor sensitivity.

Besides, the XRD results, clearly portray a huge increase in gold (220) which is parallel to gold (110) and exhibits similar behaviour. *Cheng et al.* investigation into this particular plane underscore its significance,

indicating that a high amount of Au (110) exposure leads to a decrease in anodic current compared to planes (111) and (100) [46]. While the magnitude of current generated upon glucose electrooxidation is smaller on this plane, its onset potential is much lower, offering the benefit of minimizing interference from other biomolecules.

According to the literature consulted, the impact of crystallographic orientations on glucose sensing becomes evident, offering a great study topic for enhancing sensor sensitivity, sensing potential, resistance to poisoning and selectivity.

1.6. Glucose sensing using anodized electrodes

To study the impact of Au crystallographic planes on glucose sensing, two conditions were selected. At first, 0.5M KCl was applied to 400 mC, since it showed the highest degree of increase of electroactive area and the highest reproducibility and also 0.3M KCl for 600 mC because it not only showed reproducible results but also contained different gold facets, turning it suitable for these tests.

This choice relies on the understanding that the crystallographic planes might play an important role in the sensor's sensitivity towards glucose and its poisoning from chloride ions.

As elaborated in this chapter, glucose sensing was conducted through the utilization of CV and chronoamperometry techniques. In the next subchapters, the potentials mentioned are in reference to Ag/AgCl/PBS sat..

1.6.1. CV signal study

Before assessing the glucose electrooxidation at the selected NPG electrodes an electrochemical study in buffer solutions needs to be carried out. As can be seen in Figure 17, a CV of a gold electrode was recorded in 0.1M PBS. A voltage range covering from - 0.2 V and + 1.2 V was scanned during 30 cycles.

The generated signal, presented below (Figure 17), furnishes important insights into the reactions happening between the sample and the electrolyte. From the forward scan, the presence of two peaks, A and B. The first one represents the adsorption of OH radicals and the second is associated with the formation of gold oxides. On the other hand, the peak C is attributed to the reduction of the oxides formed in B and the peak D is due to the reduction of the oxygen formed in the redox reactions during the scanning. As will be explained later, the amount of the oxides represented in peaks A and B were important for this study, since they have an impact on the electrooxidation of glucose [42].

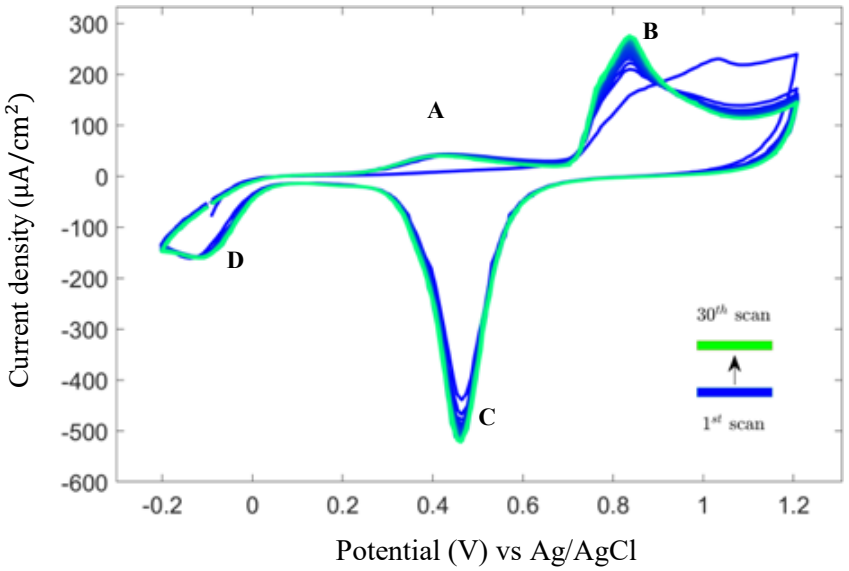

Figure 17 - CV in 0.1M PBS solution at a scan rate of 100 mV/s and a step size of 10 mV. CV recorded in the presence of a Pt wire as CE and Ag/AgCl/PBS sat. as RE.

1.6.2. Cyclic Voltammetry

To facilitate the accurate study of glucose sensing while mitigating potential contamination influences, a comprehensive electrode surface cleaning and activation process is imperative. This process serves the dual purpose of preparing the electrode surface for glucose oxidation and ensuring that the subsequent glucose measurements remain unaffected by any form of contamination.

For this, the sample was immersed in 0.1M PBS along with a platinum wire as CE, and a bridge reference filled with PBS. The replacement of 3.8M KCl with 0.1M PBS was crucial for these kinds of tests. As already mentioned, it can happen Cl^- leakage from the RE, and it was already reported by *Makovos et al.* that any type of Cl^- contamination might compromise the results. It is believed that the presence of Cl^- ions can cause Au dissolution which turns the surface electrocatalytically inactive for glucose oxidation [43].

Once the set-up preparation was concluded, a cyclic scan between - 0.2 V and + 1.2 V was performed over 30 times. As illustrated in Figure 18, the signal generated for the three samples (0.3M KCl 600 mC) has the same shape and stabilizes after a few cycles.

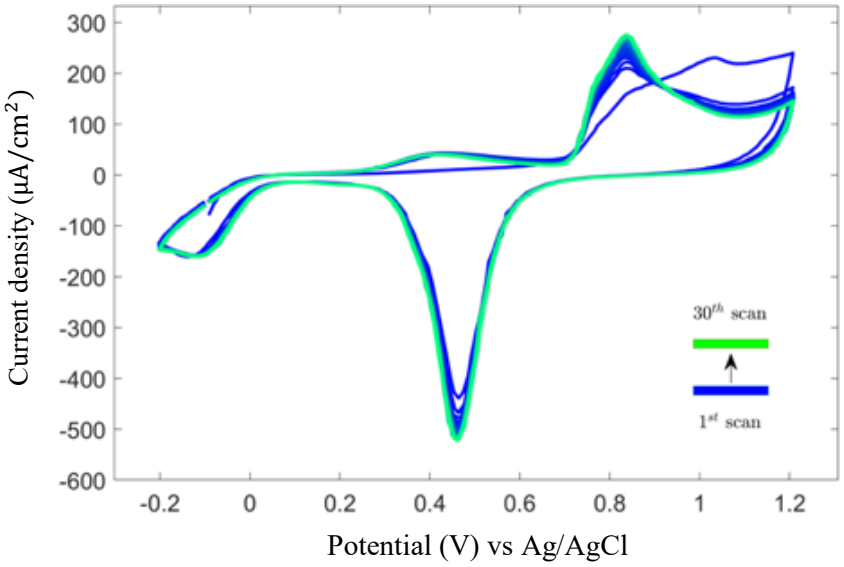

Figure 18 - CVs in 0.1M PBS solution at a scan rate of 100 mV/s and a step size of 10 mV. The signal corresponds to the electrode activation of one of the three samples prepared by chronocoulometry in 0.3M of KCl, applying a charge of 600 mC.

Afterwards, CVs were conducted, scanning three times over the same potential range. These measurements were carried out in both the absence and presence of glucose, as shown in Figure 19. For the bare PBS – Figure 19 (a) - the signal exhibited peaks at potentials of 0.85 V and 0.45 V corresponding to the oxidation and reduction of the gold oxide present in the electrode surface. However, in the presence of glucose, - Figure 17 (b) - two additional anodic peaks appear at potentials around 0.05 V and 0.3 V. These new peaks are attributed to the glucose oxidation into gluconolactone, and the oxidation of gluconolactone, respectively.

According to *Bai et al.*, glucose oxidation is dependent on the quantity of AuOH sites since they are considered active species for this reaction. Conventionally, it has been reported that at lower potentials the quantity of AuOH active sites was limited, not being enough to cause glucose oxidation. However, by following the anodization protocol developed in this project, the results show the opposite. At lower potentials, 0.05 V the active sites react with the glucose molecule originating the two-electron oxidation product (gluconolactone) [44]. In other words, it was possible to sense glucose at lower potentials, near 0 V.

Even though the outcome for this condition (0.3M KCl 600 mC) seemed reproducible, they presented an average sensitivity of (16 ± 4) $\mu A/cm^2 \cdot mM$, which was lower than the one obtained for bare gold (41 ± 4 $\mu A/cm^2 \cdot mM$, Figure 19. For the process of constructing the linear relations present in the CVs below, the data extraction was focused on the reverse scan. This selection was motivated by the reverse scan's superior stability

and more pronounced signal due to the redox reactions under consideration. The values considered to obtain the sensitivity of the anodized and bare electrodes were extracted from peaks A and B, respectively. mM

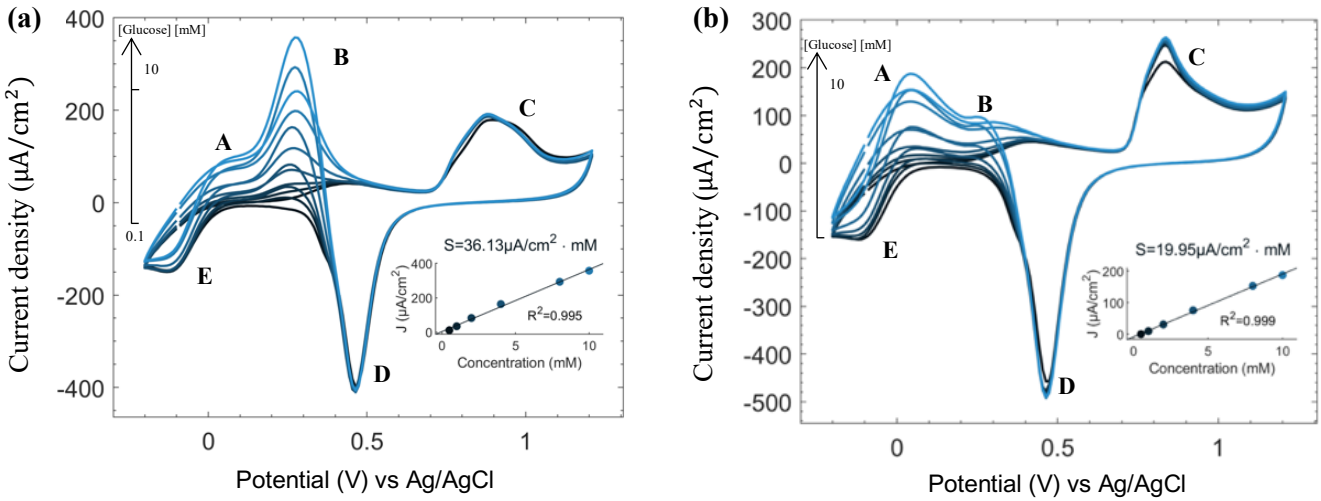

Figure 19 - CV in 0.1M PBS of (a) bare gold, and (b) anodized samples (0.3M KCl, 600 mC) in the presence of different concentrations of glucose. In the CVs the values of the sensitivity are present in the form of a linear relationship between the current density generated in the glucose activation (anodic peak in reverse scan) and the glucose concentration.

A comparative analysis of the signals presented in Figure 19 (a) and (b), corresponding to bare and anodized samples, respectively, reveal the emergence of additional peaks for the latter, as previously explained.

For a great understanding of the reaction's occurrence during the scanning, the peaks were once again denoted from letters A to E. Notably, peak B – associated with the generation of higher current density for bare gold sample - is situated at around the potential at which the formation of active hydroxide (OH) sites occurs. This confirms the influence and significance of gold hydroxide in facilitating the oxidation of glucose. Peaks C, D, and E remained unchanged showing a consistent behaviour in comparison to the signal during surface activation, meaning that the redox reactions occur at the same potentials. At peak A, as previously explained the active sites engendered during the forward scan interact with the glucose present in the solution, causing its oxidation.

Through a comparative examination of the two sets of signals (Figure 19), notable distinctions become evident. This comparative analysis highlighted variations in the potentials at which glucose was detected. Even though the sensitivity was lower for NPG, the potential at which the glucose electrooxidation was detected was lower than the already reported. Since this happens, this project presents a great novelty to be explored and applied in future devices. Besides, it also proves anodization can produce the necessary amount of AuOH sites needed for glucose sensing.

Regarding the second condition (0.5M KCl 400 mC), as evidenced by the CVs presented below (Figure 20), they exhibited a visible resemblance in signal shape across the various samples. In contrast to the other samples, these ones demonstrated an average sensitivity of ($21.3 \pm 0.7\ \mu A/cm^2 \cdot mM$). Although this sensitivity value exhibited a decrease when compared to bare gold ($41 \pm 4\ \mu A/cm^2 \cdot mM$), there was a clear shift in the potential at which the glucose was sensed (Figure 21). This shift can be regarded as a noteworthy innovation, considering that glucose detection usually occurs at higher potentials. Besides that, the uniformity in the signal shapes and sensitivity values for the three samples proves their reproducibility.

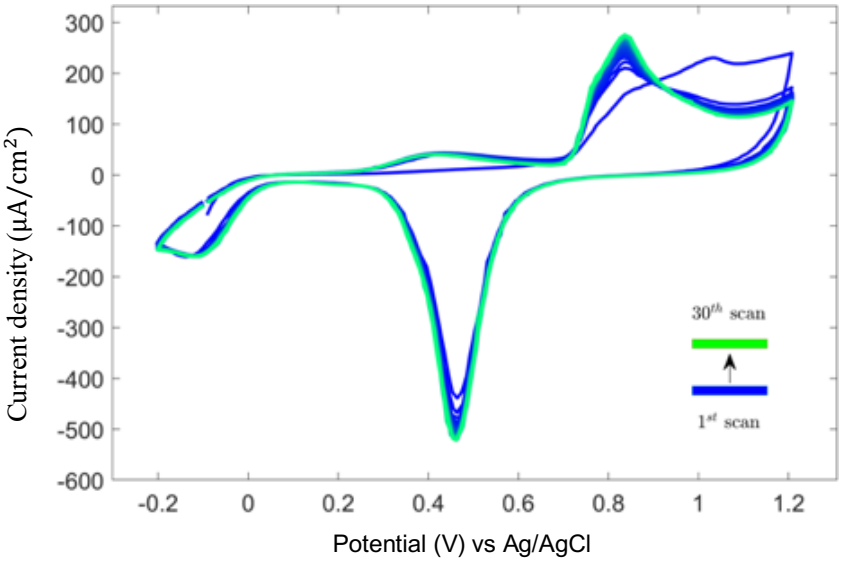

Figure 20 - CV in 0.1M PBS solution at a scan rate of 100 mV/s and a step size of 10 mV. The signals correspond to the electrode activation of one of the three samples prepared by chronocoulometry in 0.5M of KCl, applying a charge of 400 mC.

In summary, these outcomes underscore the transformative impact of the tailored anodization protocol, rendering it feasible to achieve glucose detection at considerably lower potentials, thereby contributing to the advancement of glucose sensing technologies.

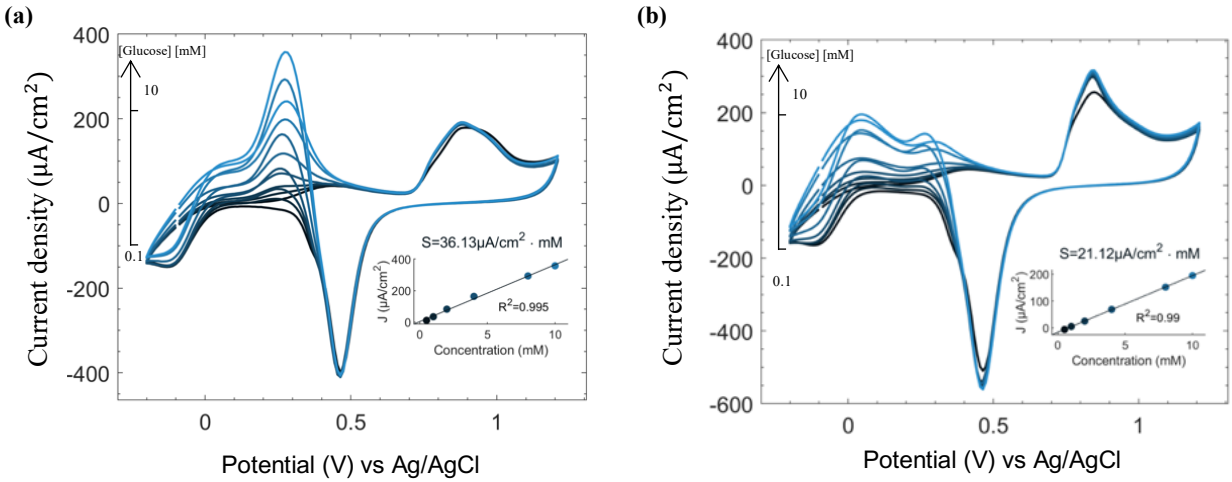

Figure 21 - CV in 0.1M PBS of (a) bare gold, and (b) anodized samples (0.5M KCl, 400 mC) in the presence of different concentrations of glucose. In the CVs, the values of the sensitivity are present in the form of a linear relationship between the current density generated in the glucose activation (anodic peak in reverse scan) and the glucose concentration.

Table 2 - Sensitivities of the bare and anodized samples obtained by CV.

Sample condition	Sensitivity [μA/cm² · mM]			Detection potential [V]
Bare Au	36.1	43.4	43.4	0.30
0.3M 600 mC	12.7	20.0	15.7	0.05
0.5M 400 mC	20.6	21.1	22.0	0.05

1.6.3. Chronoamperometry

Besides CV, chronoamperometry was also used to measure the sensitivity of the gold electrodes for glucose oxidation. For this, the study of the applied potential holds significant importance in optimizing the value to be employed in chronoamperometry.

In this subchapter, the samples considered were prepared by chronocoulometry in 0.5M KCl, applying a charge of 400 mC. As mentioned at the beginning of the chapter, this condition produced anodized samples with a greater area difference and, according to the CV analysis they presented a higher sensitivity when compared to the samples prepared in 0.3M KCl applying 600 mC.

Figure 22 (a) showcases the CVs of the activation before and after applying a potential. For the initial activation phase, the electrode was immersed in 0.1M PBS and a 30-cycle CV was recorded. This comprehensive scan encompasses a potential range from - 0.2 V to + 1.2 V vs. Ag/AgCl/PBS sat.. Subsequently, with the electrolyte under stirring conditions, 6 mM glucose was added to the system. Following 30 seconds, the defined voltage was applied until the reaction time reached 100 seconds. The behaviour of the electrode sample when the potential was applied is represented in Figure 22 (b).

To activate the gold surface again, a subsequent 3-cycle CV was recorded under the same conditions as previously described (Figure 22 (a)). It was clear that not reactivating the surface affected the electrochemical reaction and reduced the generation of current density.

By following the protocol described, the electrode regained its sensitivity to glucose. It was also instrumental to do the potential study in a sequential descent from higher to lower values. This methodological approach ensured that the oxide formed was not reduced during the experiments.

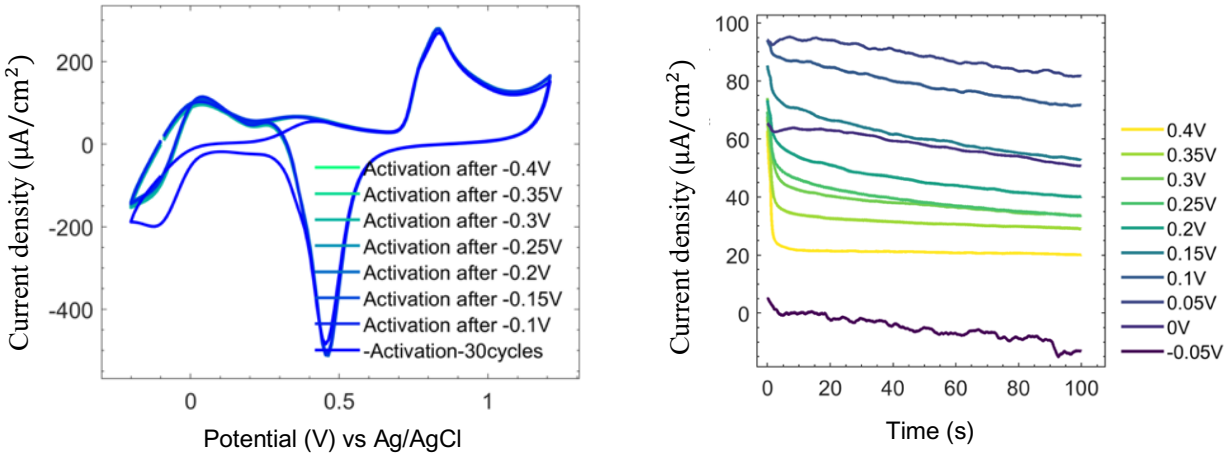

Figure 22 - (a) CVs in 0.1M PBS after the application of different applied potentials in a range from 0.1V to 0.4V vs. Ag/AgCl/KCl sat. for three scans, (b) chronoamperometry experiments at different applied potentials for 100 seconds in 0.1M PBS and 6mM glucose.

The introduction of glucose into the PBS solution led to the emergence of two additional peaks related to glucose electrooxidation at around 0.05 V and 0.3 V. Moreover, the CV displays the same behaviour after applying all the diverse potentials, meaning the glucose sensing for these nanostructured electrodes was not affected by the different applied potentials.

Even though the CV signal remained the same, in chronoamperometry (Figure 22 (b)) the potential which presented the higher current density in response to the presence of glucose was 0.05 V vs. Ag/AgCl/PBS sat. however, the stability of the signal was poor. Since it was important to have a stable signal with a great current density, 0.25 V vs. Ag/AgCl/PBS sat. was chosen as the optimal potential for the chronoamperometry tests.

After the optimization of the potential, to perform the experiments represented in Figure 23 (a), the sample was immersed in 0.1M PBS in stirring conditions (500 rpm). For these, the glucose concentration was increased in steps of 0.25mM and 1mM. Before this measurement, as usual, the Au electrode was cleaned in 0.1M PBS by scanning 30 times the potential between - 0.2 V and + 1.2 V.

The plotted data illustrates a consistent increase in the current density across all three samples upon the addition of glucose into the solution. The green linear range visible in the plots corresponds to concentrations ranging from 0.25 to 1mM of glucose, while the blue range to concentrations from 2 to 7mM

of glucose. In this context, the calibration curves express a linear trend as shown in Figure 23 (b). For higher glucose concentrations the average sensitivity obtained was (15.9 ± 0.9) $\mu A/cm^2 \cdot mM$ with a correlation coefficient of 0.996 and for lower concentrations (30 ± 4) $\mu A/cm^2 \cdot mM$ with a coefficient of 0.949. This data was obtained by averaging current values related to the plateau of each step. Subsequently, the average current values were plotted against the corresponding glucose concentration (mM). The sensitivity of each sample is represented in Table 2.

Upon a comparative analysis, it becomes evident that the sensitivity of the electrode was relatively lower for higher glucose concentrations, however, it seemed to be slightly more stable since it presented a standard deviation of 0.89 instead of 4.66 $\mu A/cm^2 \cdot mM$. This nuanced instability could likely be attributed to non-uniform anodization procedures across the various samples, exerting an undeniable influence on electrode sensing performance.

Combining all the data from the samples and both ranges, the sensitivity of the electrodes created via anodization in 0.5M KCl, utilizing a 400 mC charge via chronocoulometry, yielded an average sensitivity of (30 ± 5) $\mu A/cm^2 \cdot mM$ with a coefficient of 0.998 for lower glucose concentrations, confirming its linear behaviour of the electrode response.

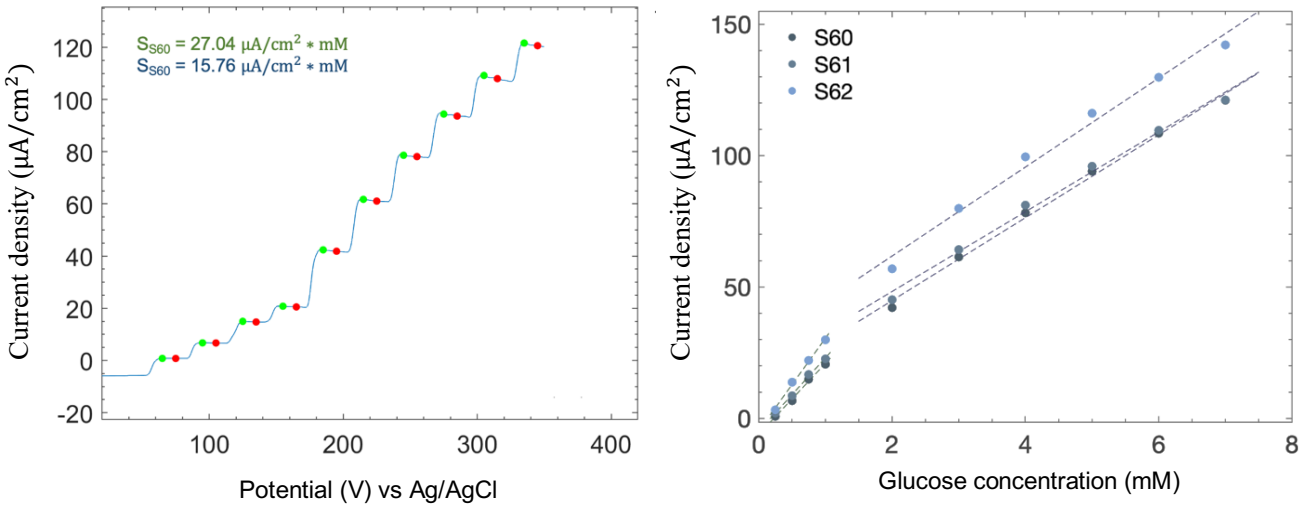

Figure 23 - Chronoamperometry measurement of the nanostructured electrodes in 0.1M PBS at a potential of +0.25V in a stirring condition of 500 rpm. Samples prepared by chronocoulometry in 0.5M KCl applying a charge of 400 mC.

For this project, and following some literature, the sensitivity to glucose was studied by chronoamperometric and voltammetric response, Table 2. As can be seen, they were not precisely the same, this discrepancy can be attributed, in part, to the conducive conditions created by continuous stirring during the amperometric measurements. This stirring promotes a more homogeneous distribution of electrolyte ions, thereby facilitating more consistent and continuous reactions at the electrode-electrolyte interface, ultimately resulting in higher current output [45]. The main reason for choosing both methods was that chronoamperometry is the technique established in literature to measure the sensitivity of the device to glucose, and CV is crucial to identify the glucose electrooxidation peaks.

The bar plot provides a concise representation of the current density generated by the NPG electrodes across a range of potentials between - 0.1 V and 0.4 V. Specifically, at potentials around 0.05 V vs. Ag/AgCl/PBS sat., the anodized sample exhibits a greater current generated, indicating an enhanced sensitivity to glucose detection at this voltage range. At higher voltages, from 0.25 V to 0.35 V, it is clear that the bare gold exhibits a higher current density towards glucose when compared to the anodized one.

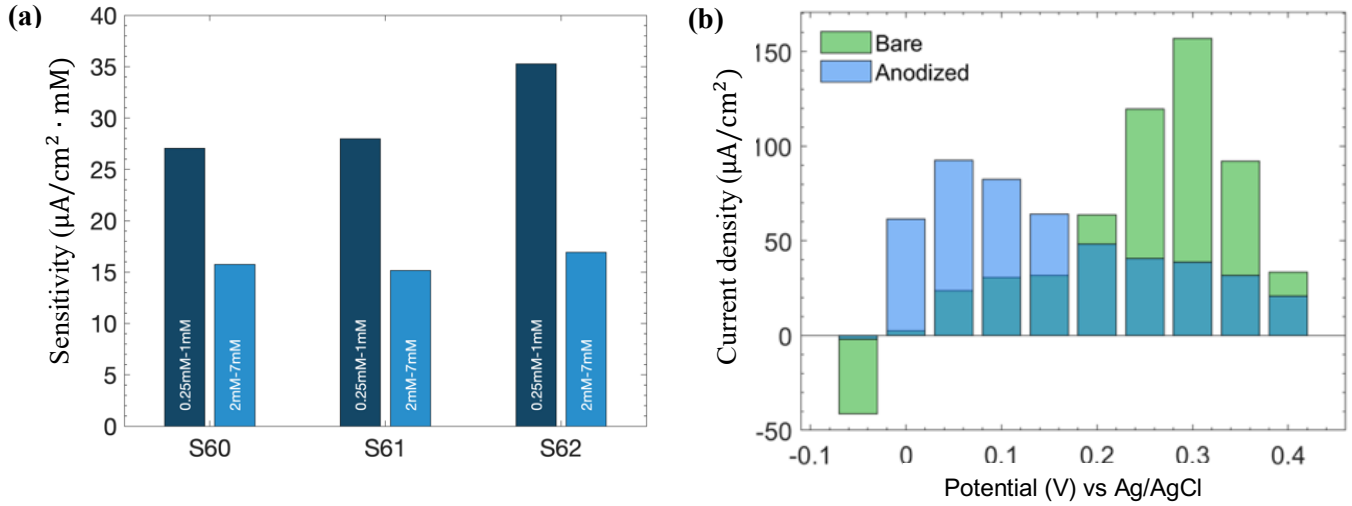

Figure 24 - (a) Sensitivities of the three nanostructured Au electrodes to glucose oxidation for different glucose concentrations (dark blue: 0.25mM – 1mM, light blue: 2mM – 7mM), obtained by chronoamperometry. (b) Comparison of the current density generated at different potentials for bare and anodized samples.

Table 3 - Sensitivity values for both samples (Bare and anodized Au) obtained by different methods, CV and chronoamperometry (CA) [0.25mM-1mM/2mM-7mM].

Sample condition	**Sensitivity [µA/cm² · mM]**			**Detection Potential [V]**
Bare Au (CV)	36.1	43.4	43.4	0.30
0.5M 400 mC - CA	27.0 / 15.7	28.0 / 15.2	35.4 / 17.0	0.05
0.5M 400 mC - CV	20.6	21.1	22.0	0.05

1.6.4. Chloride ions effect in the glucose's sensor actual response

To evaluate the influence of chloride ions on the sensing of glucose on the NPG electrodes, a CV was recorded by immersing the sample in 0.1M PBS. This study was particularly interesting since in real analysis (e.g. blood samples), chlorides are present, and it is important to understand if the electrodes are resistant to these ions.

For this study, a CV was recorded where after 50 seconds 6 mM of glucose was added to the solution. As can be seen, the bare sample in the presence of glucose generated a higher current density than the anodized sample (Figure 25). Thus, the bare sample demonstrated a higher resistance for chloride ions when compared to the anodized sample.

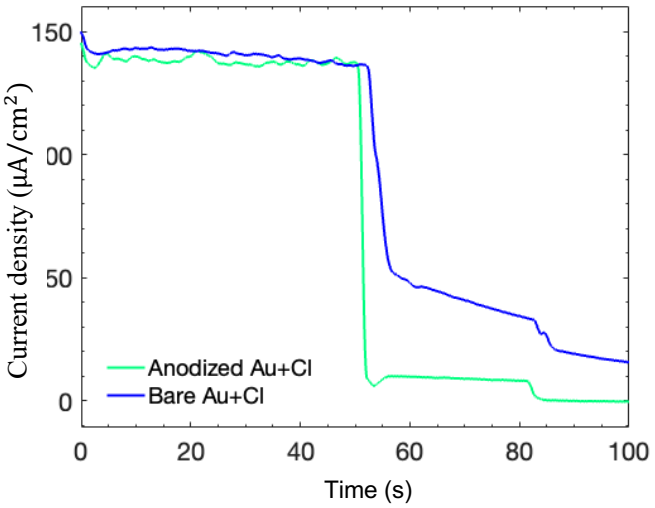

Figure 25 - Signal generated to study the influence of chloride ions in bare and anodized samples. Cyclic voltammogram in 0.1M PBS with an addition of 6 mM of glucose after 50 seconds.

Chloride ions poison the surface of the anodized samples blocking the formation of the active sites, previously proved as responsible for glucose oxidation. This occurrence could be attributed to the alterations in Au planes induced by the anodization process.

As confirmed by XRD analysis (Figure 16) there was a decrease of the preferential growth (111) after the anodization of the Au electrodes. According to *Cheng et al.*, this specific plane influences both the sensitivity of the device and the poisoning of the surface. Since there is a loss of Au (111) it is expected to have a worse surface resistance to glucose poisoning.

Figure 25 proves the influence of this plane in the poisoning of the surface. It was observable a great change in the current density for the anodized samples when compared with the bare ones, meaning the NPG was more affected by chloride poisoning.

2. Anodization on microelectrodes for impedance biosensors

As a side project for this thesis, a study of the impact of anodization in Au microelectrodes to apply in impedance biosensors was carried out.

Electrochemical impedance biosensors have been greatly studied in the literature. Its working principle bases on the application of a small amplitude AC potential to measure the phase and magnitude of the current response as a function of frequency. Besides, a conductive and biocompatible electrode is used to immobilize a biorecognition molecule, which is employed to create impedance biosensors and subsequently monitor changes in interfacial impedance brought on by analyte binding [52].

For single-cell high-throughput analysis, electrochemical impedance biosensors and microfluidic tools can be utilized to examine basic biological processes. These analytical methods can reveal biological processes at a single-cell level and identify the efficacy and toxicity of medications with high sensitivity [52].

Identifying the most recent developments in single-cell trapping technology opens up possibilities for novel structural design and technology integration. As a result, more sophisticated applications will be developed to raise measurement sensitivity to the necessary aim. In this project, the focus was on optimizing the different parameters (potential, reaction time, edge time, electrode gap distance) to obtain an efficient NPG microelectrode [52].

Various biological parameters and processes, such as glucose concentration, changes in tissue impedance, cell growth rate, toxicological analysis, and bacterial detection, among others, can be monitored by utilizing impedance as a measurable marker.

Figure 26 depicts the schematic representation of an electrochemical cell comprising two gold microelectrodes submerged in a conductive medium. C_{DL} (double-layer capacitance) represents the capacitance of the electric double layer formed at the electrode-electrolyte interface. At low frequencies, the impedance is predominantly governed by the capacitance, indicating that the accumulation and dissipation of charge at the interface are the primary factors affecting impedance behaviour. R_{sol} represents the resistance posed by the electrolyte solution. As the frequency escalates, the impedance becomes increasingly influenced by R_{sol}. Higher frequencies lead to greater penetration of current through the interface, resulting in solution resistance becoming the dominant contributor. C_{par} represents the parasitic capacitance originating from wire connections and other unintended circuit components. It adds to the total impedance of the electrochemical cell.

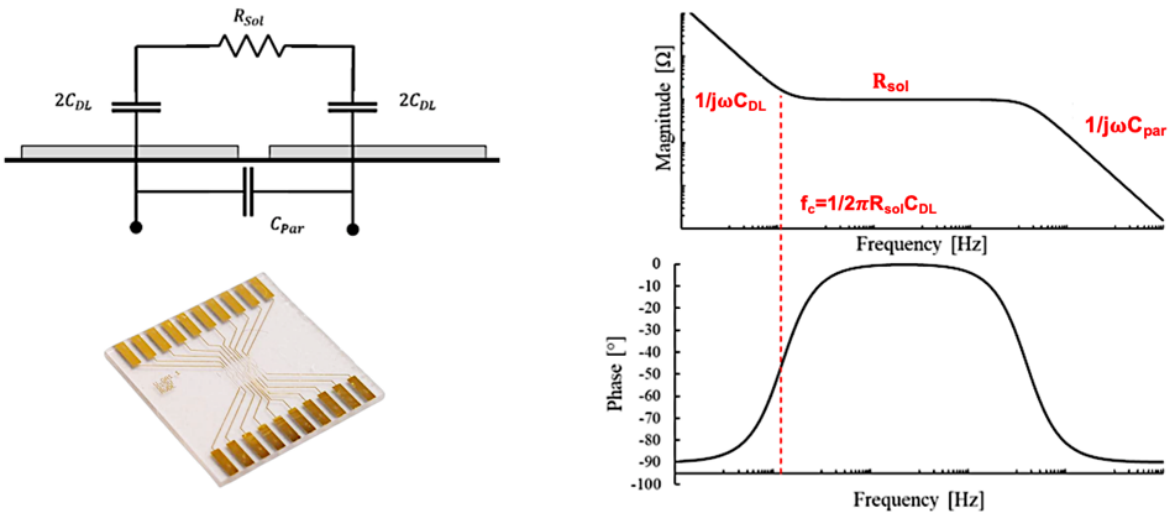

Figure 26 (a) Equivalent electric circuit of an electrochemical cell with two microelectrodes configuration [47]. (b) Bode plot of the impedance of the equivalent electric circuit. [47] Microfluidic chip produced for this project and used to optimize the reaction parameters to create an efficient NPG.

The concept of the crossover frequency (f_c) is pivotal in understanding the transition between C_{DL} and R_{sol} dominance in impedance behaviour. The crossover frequency is given by $f_c = 1/(2\pi R_{sol}C_{DL})$. Frequencies lower than f_c see C_{DL} dictating impedance, implying that the charging and discharging of the double layer exert a pronounced influence. Beyond f_c, higher frequencies entail significant current penetration through the interface, with R_{sol} assuming control over impedance characteristics [47].

In impedance biosensors where the target element for sensing exists in solution (e.g., cells or particles), detection hinges on measuring changes in R_{sol}. However, when a two-electrode system is downscaled, the crossover frequency f_c occurs at a higher frequency, constraining the bandwidth for R_{sol} measurement. This issue intrinsic to microelectrodes can be mitigated by amplifying C_{DL} to shift f_c toward lower frequencies. This approach extends the range in which R_{sol} can be effectively measured, enhancing the sensitivity and utility of impedance-based biosensing utilizing microelectrodes [47].

With the aforementioned points considered, it becomes evident that reduced impedance results in higher charge injection, thereby enhancing sensor sensitivity. At the same time, electrodes with a roughened surface exhibit amplified surface area, resulting in a significant C_{DL} and consequently, low impedance ($Z = 1/j\omega C_{DL}$).

Thus, there is a need for roughened microelectrodes. For that, the anodization process was employed since, as demonstrated in the previous chapters, it is a rapid and simple means to induce surface roughness in gold microelectrodes. This time, the electrolyte used is a PBS solution, since it showed to be capable of producing an effective roughening proved by changes in the impedance of the electrodes tested.

As the goal of this side project was to decrease the impedance of the electrode, it was imperative to assess impedance before and after implementing this technique by utilizing an impedance analyzer.

To proceed with the roughening process, an initial calibration step was required to ensure accuracy and reliability in electronic systems. During the calibration, all the microelectrodes needed to be grounded to stabilize the system. The calibration process involved an open circuit calibration, followed by a short circuit and finally a load calibration. In the last one, a resistance of 100 Ω was connected to the PCB, and then two capacitors of 100 ρF, and 10 ρF.

After completing the calibration, the impedance of the system was measured. To obtain both phase and magnitude readings, the electrode being measured should be connected to the BNC while the rest of the

electrodes were grounded. The BNC connector was used in the PCB allowing the frequency of the electrode to be read.

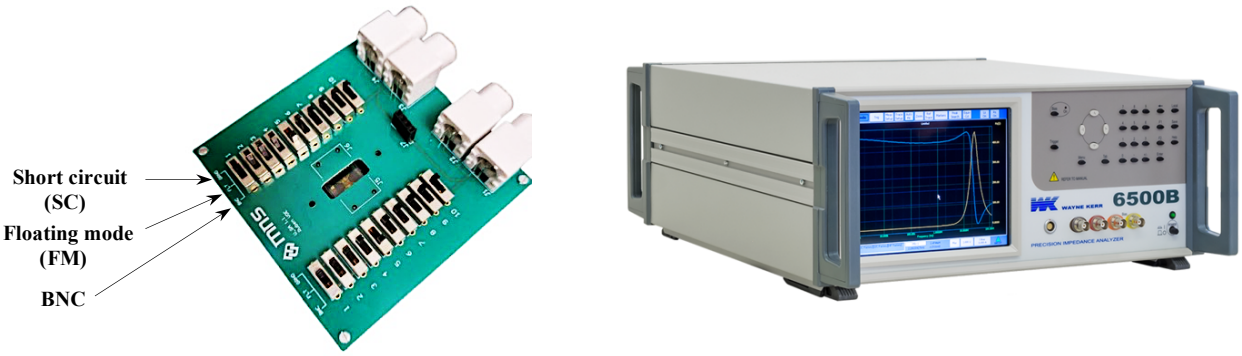

Figure 27 -Left: Set-up used in this side project. The system is composed by PCB, sample holder and sample. Right: Impedance analyzer.

For the anodization, the circuit should be connected to the function generator, and the electrodes which did not exhibit a short circuit in the previous stage should be connected to the BNC. All the other electrodes should be left in a floating mode to avoid interference in the reaction. Lastly, to monitor the impedance behaviour before and post-anodization, the PCB should be connected once again to the impedance analyzer. This process ensured that the roughening process and its effects on impedance could be accurately analyzed.

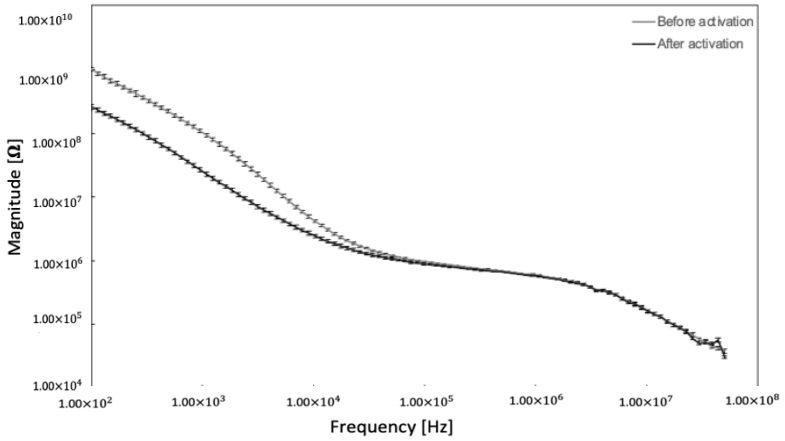

Figure 28 - Magnitude of the electrochemical cell before and after the activation, measured in 1:100 PBS solution after the application of 5 V.

Figure 28 illustrates the magnitude of the impedance before and after anodization in PBS solution, using a voltage of 5V applied for 1 second. The graph indicates that the double layer impedance was approximately three times lower after activation, corresponding to three times the value of C_{DL} initially observed. This difference can be calculated by different approaches, for this project the relation $|Z|=1/C_{DL}$ was used. With the value of the magnitude extracted from the bode plot (Figure 30), it was possible to obtain the C_{DL}.

Lastly, the overlapping of the curves at higher frequencies suggested that R_{Sol} and C_{par} remained unchanged between measurements.

To explore the impact of different voltages on electrode roughening and its effects on impedance, a range of potentials were tested as shown in Figure 29. The voltages 5V, 8V, 10V and 16V were studied, with the same experimental protocol previously described. This investigation aimed to understand how varying the

applied voltage influences the roughening process and subsequently affects the impedance characteristics of the electrode.

Figure 29 illustrates a clear trend where the impedance of the microelectrodes decreased almost proportionally with the applied potential. This observation suggested that higher applied potentials led to lower impedance values and greater double-layer capacitance. In simpler terms, increasing the applied potential results in a rougher electrode surface. For this project, an average of 15 electrodes per potential were tested after anodization, and approximately 75 electrodes before any treatment.

The roughening process of the electrodes is thought to be driven by the electrochemical reaction between Au and Cl^- ions [48]. When a specific voltage is applied, Au reacts with Cl^- ions and undergoes partial etching, resulting in the formation of a roughened surface. This surface modification was linked to changes in the double-layer capacitance and impedance characteristics, which can be crucial for enhancing the sensitivity and performance of the microelectrodes in various applications, including biosensing.

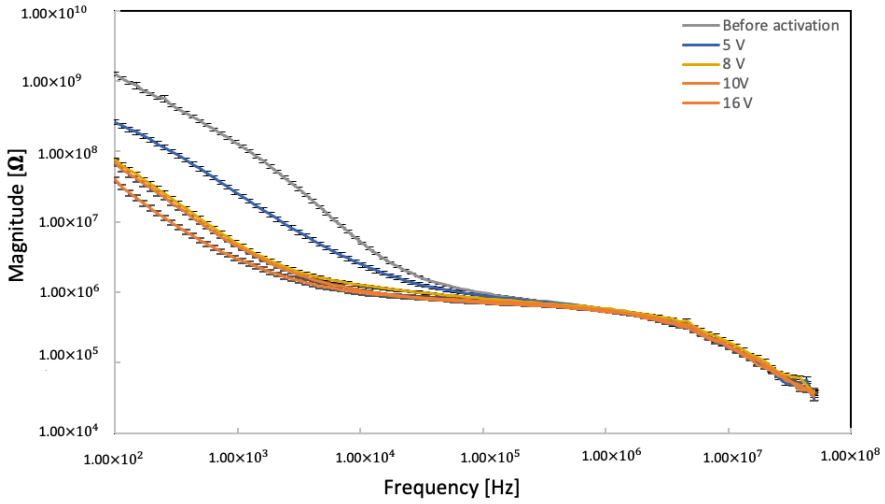

Figure 29 - Magnitude of the electrochemical cell before and after the activation, measured in 1:100 PBS solution after the application of 5, 8, 10 and 16 V.

Even though multiple parameters can be fine-tuned to optimize the roughening technique, such as the electrode gap, Cl^- ions content in the electrolyte, applied potential, and reaction time, this protocol demonstrates a successful approach to decrease the impedance of the electrodes and enhance the sensor sensitivity for single cell detection. By applying 5 V the impedance decreased in 3 times when compared to the bare samples, for 8 V and 10 V about 14 times and for 16 V around 33 times, measured at a frequency of 1×10^2 Hz.

According to the results obtained 16 V should be the optimum applied potential since it produced a greater change in the area, however by microscopy analysis, it was possible to see the microelectrodes were destroyed, meaning the anodization in these conditions was too intense. Since this happened, 10 V was defined as the ideal voltage since it produced a great NPG without destroying the electrode itself.

Furthermore, the outcomes emphasize the flexibility of the anodization technique. By changing some parameters, such as electrolyte type, concentration and applied potential, the technique was capable of producing an efficient nanoporous structure with enhanced properties for diverse applications.

4

CONCLUSION AND FUTURE PERSPECTIVES

Over the past decades, diabetes has shown exponential growth all over the world, reaching over 440 million cases. As this happens, the early-stage detection of diseases can play an important role in both, patient health and the reduction of treatment costs.

At this point, researchers' main focus is based on reaching a continuous and real-time measurement of clinically relevant molecules and developing implantable and point-of-care (POC) devices. However, the traditional glucose sensing methods present some limitations in terms of accuracy, selectivity, sensitivity, and response time.

To address these challenges, researchers have turned their attention to developing advanced electrochemical glucose sensors. For this, it is crucial to create and use an efficient electrode and among the various materials, gold has shown great promise due to its excellent conductivity, stability, biocompatibility and capability to electrooxidize glucose without the mediation of an enzyme.

By roughening the electrode surface, in this case, gold, the sensitivity of the device to glucose can be increased as well and the fouling can be reduced due to the effect of chloride ions.

For this project, as a quick, simple, low-cost, and user-friendly technique, anodization has been explored. Besides the qualities listed, this method has shown a great possibility of creating a nanostructured gold electrode to sense glucose without the interference of any other molecules. As reported, anodization can control and create different gold crystallographic planes which have been shown to play an important role in the sensitivity, selectivity and resistance to chloride ions poisoning when sensing glucose.

As discussed in the previous chapter, a robust procedure to fabricate nanostructured macroelectrodes were developed by using chronocoulometry in diluted KCl within 15 seconds. To characterize the electrode's ability to sense glucose several techniques were used, such as CV and chronoamperometry. XRD and SEM were employed for the understanding of the crystal and structural properties of the developed electrodes.

By recording CV and chronoamperometry in 0.1M PBS, the anodized samples have shown to be able to sense glucose oxidation presenting a sensitivity of 21.3 $\mu A/cm^2 \cdot mM$ using CV (0.1-10 mM glucose), and 30.1 and 16 $\mu A/cm^2 \cdot mM$ using chronoamperometry for glucose concentrations of 0.25-1mM and 2-7mM, respectively. By the chronoamperometry analysis, the electrodes show a better sensitivity for lower glucose concentrations, more specifically, a range between 0.25 and 1mM. In other words, the anodized electrodes have a good capacity to sense glucose when the sample is diluted.

The main novelty of this project is the fact that the sensing of glucose occurs at lower potentials than what was never previously reported, happening at voltages of around 0.05 V vs. Ag/AgCl. Detecting glucose at low potentials can offer several advantages in the context of glucose sensors for medical and physiological monitoring. One of the key benefits is the reduced signal interferences since low potentials often result in reduced electrooxidation of other electroactive species present in, for example, blood samples. Knowing this, by operating at this voltage range, the sensor can minimize the cross-reactivity with other substances, leading to more accurate readings.

As it decreases the interference of other biomolecules, the specificity of the sensor will increase since it will respond primarily to glucose, improving its specificity.

Besides all of these benefits, operating at low potentials is considered less harmful to living tissues and cells, meaning this feature can enhance the biocompatibility of the sensor, minimizing the potential for tissue damage or adverse reactions.

Lastly, low potentials are also beneficial for long-term sensors, such as implantable or wearable devices since the power requirements of the sensor are low.

In conclusion, the results show that is possible to produce a device which can be capable of sensing glucose with a higher selectivity, biocompatible, safe for the user, and with a long lifetime.

The results also present some drawbacks, such as the fact the optimized NPG shows a lower sensitivity than the bare gold. During the anodization, it was clear that the colour change was not uniform along the sample which means that the anodization requires further optimization such as imposing a stirring condition during the process itself or changing the type of counter electrode (e.g., flat or cylindrical mesh placed exactly in front of the sample). Replacing a wire electrode for a mesh counter can present some benefits since it has a higher surface area which can lead to an enhanced mass transport of the ions leading to a uniform current distribution that at the same time will produce a higher current density.

Finally, a different variation of the protocol can impose a high constant temperature during anodization since it has been proved that increasing this reaction parameter produced gold electrodes with higher roughness factors [53].

By exploring these changes, the NPG electrodes should be capable of sensing glucose at lower potentials enhancing several features of these continuous glucose monitoring sensors, such as selectivity, specificity, biocompatibility and energy efficiency.

Regarding microelectrodes, anodization has shown to be capable of roughening not only at the macro but also microscale. It produced nanoporous microelectrodes to apply in impedance electrochemical biosensors. As explained, after anodization microelectrodes presented a lower impedance, meaning a higher C_{DL} which allows the trapping of a single cell.

Besides producing great results in microfabrication, this project proved the tunability of the anodization since by changing some parameters, in this case, electrolyte and potential, the roughening still happens and can produce roughening at different scales to use in diverse applications and different targets.

REFERENCES

[1] Anik, U. (2017). Electrochemical medical biosensors for POC applications. In Medical Biosensors for Point of Care (POC) Applications (pp. 275–292). Elsevier Inc. https://doi.org/10.1016/B978-0-08-100072-4.00012-5

[2] N. G. Costa, J. C. Antunes, A. J. Paleo, and A. M. Rocha, "A Review on Flexible Electrochemical Biosensors to Monitor Alcohol in Sweat," Biosensors, vol. 12, no. 4. MDPI, Apr. 01, 2022. doi 10.3390/bios12040252.

[3] Singh, A., Sharma, A., Ahmed, A., Sundramoorthy, A. K., Furukawa, H., Arya, S., & Khosla, A. (2021). Recent advances in electrochemical biosensors: Applications, challenges, and future scope. In Biosensors (Vol. 11, Issue 9). MDPI. https://doi.org/10.3390/bios11090336

[4] IUPAC. Compendium of Chemical Terminology, 2nd ed. (the "Gold Book"). Compiled by A. D. McNaught and A. Wilkinson. Blackwell Scientific Publications, Oxford (1997). Online version (2019-) created by S. J. Chalk. ISBN 0-9678550-9-8.

[5] Cui, F., Zhou, Z., & Zhou, H. S. (2020). Review—Measurement and Analysis of Cancer Biomarkers Based on Electrochemical Biosensors. Journal of The Electrochemical Society, 167(3), 037525. https://doi.org/10.1149/2.0252003jes

[6] Grieshaber, D., Mackenzie, R., Vörös, J., & Reimhult, E. (2008). Electrochemical Biosensors-Sensor Principles and Architectures. Sensors, 8, 1400–1458. www.mdpi.org/sensors

[7] Lyons, C., Clark, L. C., Mcdowell, H., & Mcarthur, K. (1964). ANNALS OF SURGERY: Cerebral Venous Oxygen Content During Carotid Thrombintimectomy.

[8] Guilbault, George G., et al. "Use of Ion Selective Electrodes in Enzymic Analysis. Cation Electrodes for Deaminase Enzyme Systems." Analytical Chemistry, vol. 41, no. 4, 1 Apr. 1969, pp. 600–605, https://doi.org/10.1021/ac60273a016.

[9] Singh, Simranjeet, et al. "Biological Biosensors for Monitoring and Diagnosis." Environmental and Microbial Biotechnology, 2020, pp. 317–335, https://doi.org/10.1007/978-981-15-2817-0_14.

[10] Cho, I. H., Kim, D. H., & Park, S. (2020). Electrochemical biosensors: Perspective on functional nanomaterials for on-site analysis. In Biomaterials Research (Vol. 24, Issue 1). BioMed Central Ltd. https://doi.org/10.1186/s40824-019-0181-y

[11] Rempel, A. A. (2007). Nanotechnologies. Properties and applications of nanostructured materials. Russian Chemical Reviews, 76(5), 435–461. https://doi.org/10.1070/rc2007v076n05abeh003674

[12] Rafique, M., Tahir, M. B., Rafique, M. S., Safdar, N., & Tahir, R. (2020). Nanostructure materials and their classification by dimensionality. Nanotechnology and Photocatalysis for Environmental Applications, 27–44. https://doi.org/10.1016/B978-0-12-821192-2.00002-4

[13] Zhang, R., & Olin, H. (2014). Porous gold films short review on recent progress. In Materials (Vol. 7, Issue 5, pp. 3834–3854). MDPI AG. https://doi.org/10.3390/ma7053834

[14] He, K., Jiang, Y., Wang, T., Liu, Z., Wang, M., Pan, L., & Chen, X. (2022). Assemblies and composites of gold nanostructures for functional devices. Aggregate, 3(4). https://doi.org/10.1002/agt2.57

[15] P. Bollella, "Porous Gold: A New Frontier for Enzyme-Based Electrodes", doi: 10.3390/nano10040722.

[16] Razali, M. H., & Ismail, N. A. (2021). Basic concepts and processing of nanostructured materials. Nanoscale Processing, 1–32. https://doi.org/10.1016/B978-0-12-820569-3.00001-3

[17] Y. Mie, Y. Yasutake, M. Ikegami, and T. Tamura, "Anodized gold surface enables mediator-free and low-overpotential electrochemical oxidation of NADH: A facile method for the development of an NAD+-dependent enzyme biosensor," Sens Actuators B Chem, vol. 288, pp. 512–518, Jun. 2019, doi: 10.1016/J.SNB.2019.03.039.

[18] Minju Kim and Jongwon Kim. (2014). Effect of pH on Anodic Formation of Nanoporous Gold Films in Chloride Solutions: Optimization of Anodization for Ultrahigh Porous Structures. American Chemical Society, 30, 4844–4851. https://doi.org/10.1021/la500732z

[19] Sáenz, H. S. C., Hernández-Saravia, L. P., Selva, J. S. G., Sukeri, A., Espinoza-Montero, P. J., & Bertotti, M. (2018). Electrochemical dopamine sensor using a nanoporous gold microelectrode: a proof-of-concept study for the detection of dopamine release by scanning electrochemical microscopy. Microchimica Acta, 185(8). https://doi.org/10.1007/s00604-018- 2898-z

[20] Tavakkoli, N., Soltani, N., & Mohammadi, F. (2019). A nanoporous gold-based electrochemical aptasensor for sensitive detection of cocaine. RSC Advances, 9(25), 14296–14301. https://doi.org/10.1039/c9ra01292c

[21] Yao, C., Lu, J., & Webster, T. J. (2011). Titanium and cobalt–chromium alloys for hips and knees. Biomaterials for Artificial Organs, 34–55. https://doi.org/10.1533/9780857090843.1.34

[22] Lee, W., & Park, S. J. (2014). Porous anodic aluminium oxide: Anodization and templated synthesis of functional nanostructures. In Chemical Reviews (Vol. 114, Issue 15, pp. 7487–7556). American Chemical Society. https://doi.org/10.1021/cr500002z

[23] C. Karunakaran, R. Rajkumar, and K. Bhargava, "Introduction to Biosensors," Biosens Bioelectron, pp. 1–68, Jan. 2015, doi: 10.1016/B978-0-12-803100-1.00001-3.

[24] Xu, J., Kou, T., & Zhang, Z. (2013). Anodization strategy to fabricate nanoporous gold for high-sensitivity detection of p-nitrophenol. CrystEngComm, 15(39), 7856–7862. https://doi.org/10.1039/c3ce40880a

[25] Nishio, K., & Masuda, H. (2011). Anodization of gold in oxalate solution to form a nanoporous black film. Angewandte Chemie - International Edition, 50(7), 1603–1607. https://doi.org/10.1002/anie.201005700
[26] Netzahualcóyotl Arroyo-Currás, Karen Scida, Kyle L. Ploense, Tod E. Kippin, & Kevin W. Plaxco. (2017). High Surface Area Electrodes Generated via Electrochemical Roughening Improve the Signaling of Electrochemical Aptamer-Based Biosensors. American Chemical Society, 89, 12185–12191. https://doi.org/10.1021/acs.analchem.7b02830
[27] Sukeri, A., Saravia, L. P. H., & Bertotti, M. (2015). A facile electrochemical approach to fabricate a nanoporous gold film electrode and its electrocatalytic activity towards dissolved oxygen reduction. Physical Chemistry Chemical Physics, 17(43), 28510–28514. https://doi.org/10.1039/c5cp05220c
[28] Sadeghi, M., & Shabani-Nooshabadi, M. (2022). Use of a nano-porous gold film electrode modified with chitosan/polypyrrole for electrochemical determination of metronidazole in the Presence of Acetaminophen. Chemosphere, 307. https://doi.org/10.1016/j.chemosphere.2022.135722
[29] Bard, A. J., et al. (2019). Electrochemical Methods: Fundamentals and Applications (3rd ed.). John Wiley & Sons.
[30] Lamy, C., et al. (2009). Structure Sensitivity of Glucose Oxidation on Gold Single Crystal Electrodes. Journal of the American Chemical Society, 131(22), 7990-8002.
[31] Kelaidopoulou, A., Papoutsis, A., Kokkinidis, G., Napporn, W. T., Leger, J.-M., & Lamy, C. (1998). Electrooxidation of b-D(+)glucose on bare and u.p.d. modi®ed platinum particles dispersed in polyaniline.
[32] Elgrishi, N., Rountree, K. J., McCarthy, B. D., Rountree, E. S., & Eisenhart, T. T. (2018). Cyclic voltammetry: An introduction. Journal of Chemical Education, 95(2), 197-206.
[33] Bard, A. J., & Faulkner, L. R. (2001). Electrochemical Methods: Fundamentals and Applications (2nd ed.). Wiley
[34] Kissinger, P. T., & Heineman, W. R. (1983). Cyclic Voltammetry. Journal of Chemical Education, 60(9), 702-706.
[35] Lv, H., Pan, Q., Song, Y., Liu, X. X., & Liu, T. (2020). A Review on Nano-/Microstructured Materials Constructed by Electrochemical Technologies for Supercapacitors. In Nano-Micro Letters (Vol. 12, Issue 1). Springer. https://doi.org/10.1007/s40820-020-00451-z
[36] Kamat, P. V., Datta, A., El-Sayed, M. A., Hartland, G. V., Kuroda, P. K., Rodgers, M. A. J., ... & Zou, S. (2010). Photophysical, photochemical and photocatalytic aspects of metal nanoparticles. Chemical Reviews, 110(2), 1887-1918.
[37] El Harrad, L., Chazalviel, J. N., & Ozanam, F. (2018). Two-step chronoamperometry in thin layer electrochemistry. Journal of Electroanalytical Chemistry, 819, 287-296.
[38] Mohd Zaki, M. H., Mohd, Y., & Chin, L. Y. (2020). Surface Properties of Nanostructured Gold Coatings Electrodeposited at Different Potentials. International Journal of Electrochemical Science, 15(11), 11401–11415. https://doi.org/10.20964/2020.11.41
[39] Gallego, J. H., Castellano, C. E., Calandra, A. J., & Arvia, A. J. (1975). The electrochemistry of gold in acid-aqueous solutions containing chloride ions. Journal of Electroanalytical Chemistry and Interfacial Electrochemistry, 66(3), 207–230. https://doi.org/10.1016/S0022-0728(75)80004-0
[40] Diaz, M. A., Kelsall, G. H., & Welham, N. J. (1993). Electrowinning coupled to gold leaching by electrogenerated chlorine: I. Au(III)□Au(I) / Au kinetics in aqueous Cl2/Cl− electrolytes. Journal of Electroanalytical Chemistry, 361(1–2), 25–38. https://doi.org/10.1016/0022-0728(93)87035-T
[41] Nishio, Kazuyuki, and Hideki Masuda. "Formation of Nanoporous Anodic Gold Oxide Films in Carboxylic Acids and Spontaneous Reduction to Nanoporous Gold." Bulletin of the Chemical Society of Japan, vol. 86, no. 10, 15 Oct. 2013, pp. 1144–1150, https://doi.org/10.1246/bcsj.20130142.
[42] Podestá, J. J., Piatti, R. C. V., & Arvía, A. J. (1979). Periodic current oscillations at the gold/acid aqueous interfaces induced by HCl additions. Electrochimica Acta, 24(6), 633–638. https://doi.org/10.1016/0013-4686(79)87044-9
[43] Makovos, E. B., & Liu, C. C. (1986). A cyclic-voltammetric study of glucose oxidation on a gold electrode. Bioelectrochemistry and Bioenergetics, 15(2), 157–165. https://doi.org/10.1016/0302-4598(86)80023-X
[44] Bai, Y., Yang, W., Sun, Y., & Sun, C. (2008). Enzyme-free glucose sensor based on a three-dimensional gold film electrode. Sensors and Actuators B: Chemical, 134(2), 471–476. https://doi.org/10.1016/J.SNB.2008.05.028
[45] Cherevko, S., & Chung, C. H. (2009). Gold nanowire array electrode for non-enzymatic voltammetric and amperometric glucose detection. Sensors and Actuators B: Chemical, 142(1), 216–223. https://doi.org/10.1016/J.SNB.2009.07.023
[46] Cheng, T. M., Huang, T. K., Lin, H. K., Tung, S. P., Chen, Y. L., Lee, C. Y., & Chiu, H. T. (2010). (110)-Exposed gold nanocoral electrode as low onset potential selective glucose sensor. ACS Applied Materials and Interfaces, 2(10), 2773–2780. https://doi.org/10.1021/am100432a
[47] van den Eeckhoudt, R., Rusli, N. I., Boon, N., Tavernier, F., Taurino, I., & Kraft, M. (n.d.). In situ roughening of gold microelectrodes for increased bandwidth of single cell impedance biosensors.
[50] Cherevko, S., Topalov, A. A., Zeradjanin, A. R., Katsounaros, I., & Mayrhofer, K. J. J. (2013). Gold dissolution: Towards an understanding of noble metal corrosion. *RSC Advances*, *3*(37), 16516–16527. https://doi.org/10.1039/c3ra42684j
[51] World Health Organization. *Global Health Risks: Mortality and Burden of Disease Attributable to Selected Major Risks*; World Health Organization: Geneva, Switzerland, 2009.
[52] Radhakrishnan, R., Suni, I. I., Bever, C. S., & Hammock, B. D. (2014). Impedance biosensors: Applications to sustainability and remaining technical challenges. *ACS Sustainable Chemistry and Engineering*, *2*(7), 1649–1655. https://doi.org/10.1021/sc500106y
[53] Kim, M., Jeong, H., Lee, E., & Kim, J. (2015). Effect of temperature and chloride concentration on the anodic formation of nanoporous gold films in chloride solutions. *Bulletin of the Korean Chemical Society*, *36*(9), 2337–2343. https://doi.org/10.1002/bkcs.10463

A
APPENDIX

During the first experiments, the electrochemical measurement of the samples' area was not effective. As a result, a 5% difference in the initial area was observed when comparing samples from the same wafer. During these investigations, several crucial precautions and considerations were identified, and these will be thoroughly examined in this chapter.

1.4.1 Photoresist layer

The first samples tested that showed this significant difference in the electrochemical area were prepared without a photoresist layer on top. As a photoresist (PR) layer is used several times to protect the substrates, later, to compare the different behaviours, some samples with on top *S1818* PR were tested.

During the experiments, the samples with PR have shown to be better ensuring gold adhesion to the glass (Figure A1). This comes not only for the protection of this layer but also for the existence of an additional layer (Titanium), and also for the optimization of the deposition parameters.

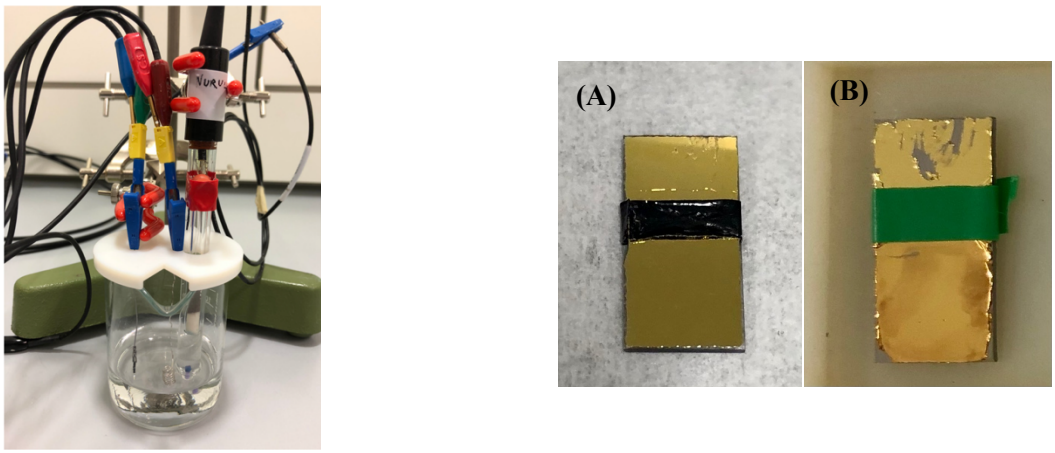

Figure A1 – (left) Set-up used for all the experiments. (right) Samples state after anodization (A) with, (B) without a photoresist layer.

Besides that, the resulting CVs of the samples where the PR layer was not present, have shown much higher levels of contamination and instability on both, reduction and oxygen peaks, and also on the double-layer region (Figure A2).

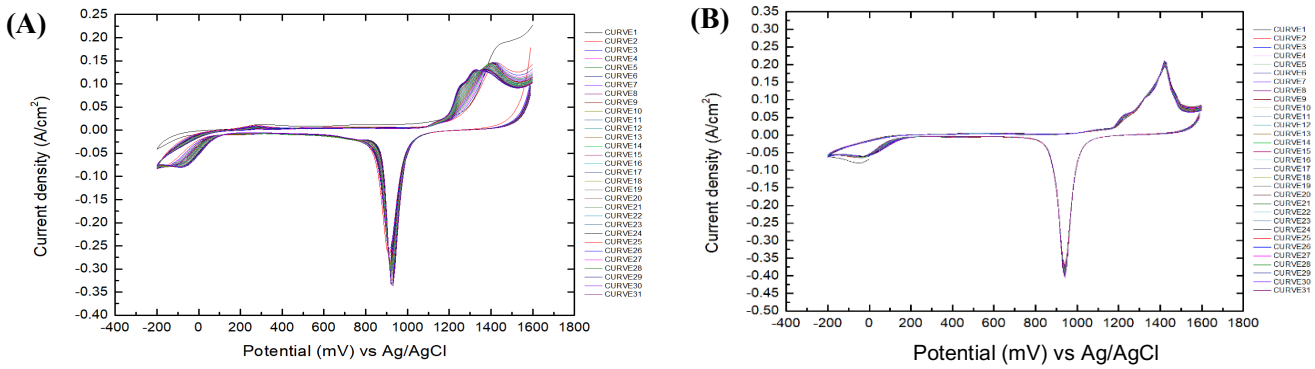

Figure A2 – CVs of samples (A) without, (B) with a photoresist layer.

This contamination may come from different factors, either by touching the samples with gloves or by air contamination since the samples were not stored in vacuum boxes. A *PR* layer was proven to be a valuable solution to prevent this issue.

1.4.2 Chloride leakage

At first, when using the reference filled with 3.8M KCl, the results showed an additional reduction peak at around 0.75 V vs. Ag/AgCl/ H_2SO_4 sat., which compromised the measurement of the electroactive area (overestimation).

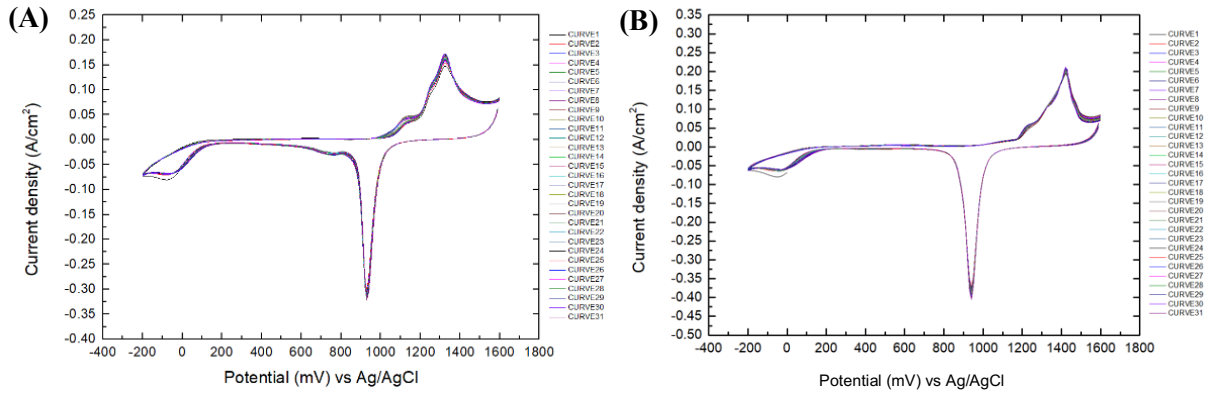

Figure A3 - CVs using a triple junction electrode filled with 3.8M KCl (A), and a bridge (B) in 0.5M H_2SO_4.

One reason to justify this second peak (Figure A3 (A)) is chloride release from the RE that, at the same time contaminates the beaker solution is etching the gold from the working electrode via the formation of gold chloride complexes [23].

As evident from the provided data, this effect will complicate determinations of the electrode's electrochemical surface area from CVs [24] [35].

To solve this issue, a bridge reference filled with 0.5M H_2SO_4 was used, eliminating the chloride leakage effects. In these CVs, it is observable that the second reduction peak disappears, and the peak that occurred at around 0.90 V vs. Ag/AgCl/ H_2SO_4 sat. maintained unchanged. The fact the reduction at 0.75 V vs. Ag/AgCl/ H_2SO_4 sat. has vanished, indicates the bridge electrode could solve the problem and the gold was not being etched and re-deposited by chloride ions.

Besides solving the problem, with the data presented, can be proved that in fact the effect seen was caused by chloride ions that interfered with the measurement and characterization of the surface area.

1.4.3 Electrode position

The position of the electrodes is also shown to have an impact on the signal detected, as evident in the CVs in Figure A4.

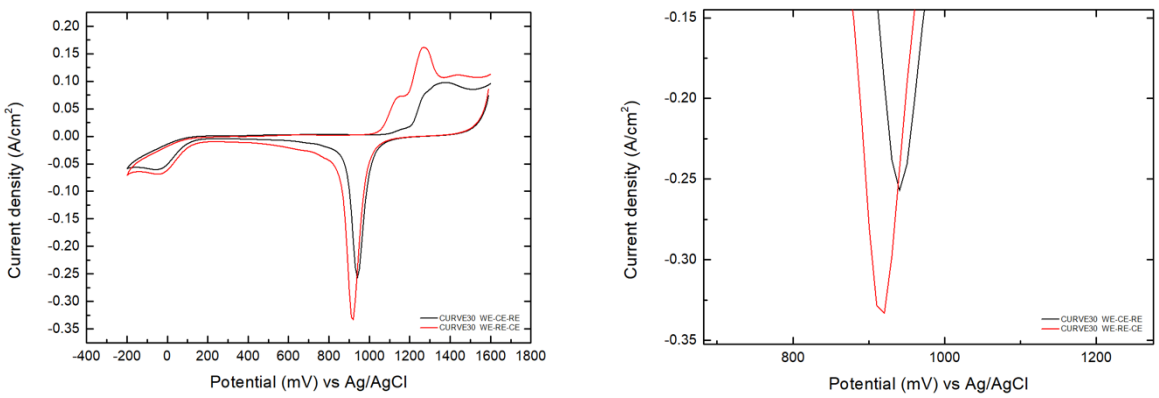

Figure A4 - CVs of measurements placing the CE in the center, black line, or in one extreme, red line.

The reduction peak shifted to the right, changing the potential where the reduction reaction happened, from 0.90 V to 0.98 V vs. Ag/AgCl/ H_2SO_4 sat.. By changing the CE position from the extreme to the center, near the WE, the signal showed to be more stable and precise in measuring the electrode area. This happened because the WE should always be placed parallel to the RE and close to the CE, to guarantee the signal measured is analyzing the fulfilled reaction.

Besides this, it is important to maintain the RE position, otherwise a similar shift will appear on the signal. To solve this problem and guarantee the electrodes are always at the same distance, a cap was designed in *SolidEdge* and 3D printed, Figure A5. During the experiments, this cap was shown to be a great approach to solving this issue.

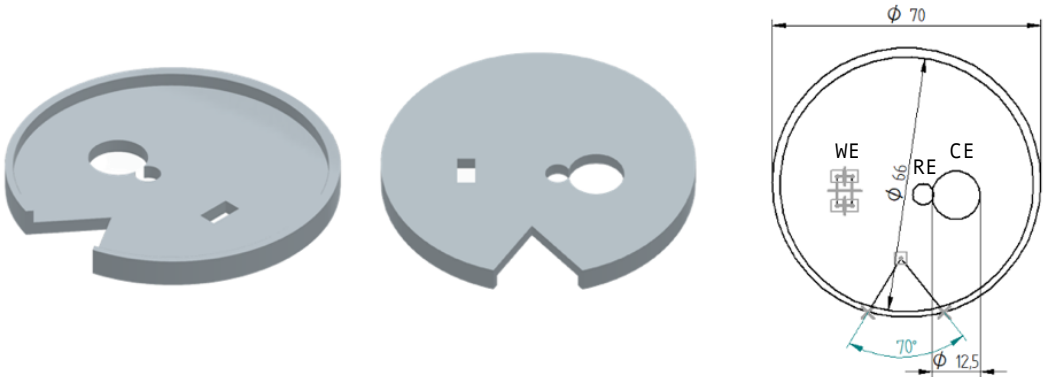

Figure A5 – Cap design produced in the software *SolidEdge*.

1.4.1 Electrode aligner

Another topic that plays an important role in this procedure is the sample preparation. To ensure every sample had the same area a tape aligner was designed.

For the first samples, some differences in the active area of the electrodes were detected which compromised the data from the beginning.

When producing the electrode aligner, Figure A6, was instrumental to have a strip of tape or other material completely straight. Besides this, the user should be able to carefully adhere the tape to the sample. If this last caution is not fulfilled, during the experiments the electrolyte solution will go underneath the tape and start a non-desired reaction which will affect the results.

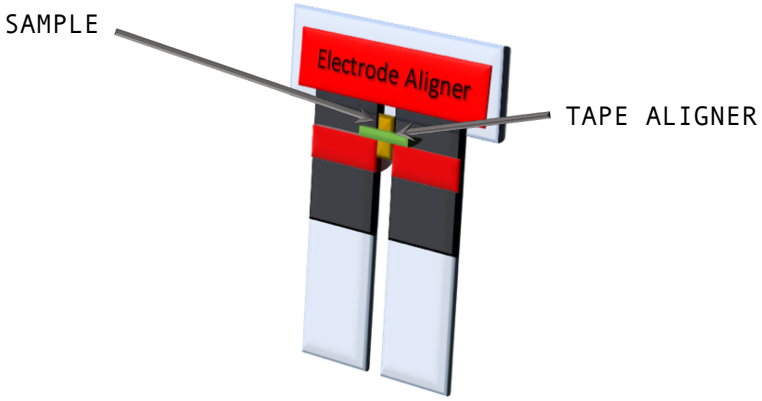

Figure A6 - Electrode aligner used to prepare the samples.

As this happened, the device produced at the end had shown to be suitable for this project since it was simple and easy to prepare, ensured the samples had the same area and also presented no problem in pressing the tape to adhere to the sample.

1.4.2 Conductive area

Lastly, the first cyclic voltammograms obtained were also compromised by some instability in the active area. The data presented in Figure A7 shows some peaks which might be coming from tantalum dissolution. This happens due to the fact the active area in contact with the clip is not completely dry. It might mean there is some remaining solution in this region which can cause this undesired reaction provoking the dissolution of the clip.

As mentioned, this problem should be solved by guaranteeing the active area is not scratched and completely dry before every test.

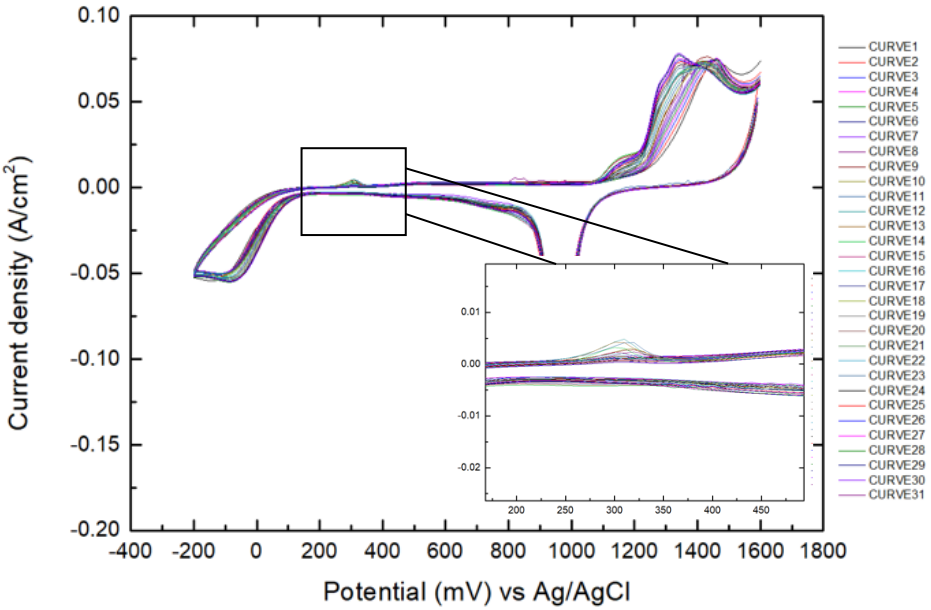

Figure A7 - CVs of samples with the contact area wet or contaminated.

B
APPENDIX

Table A1 - Conditions used in the cyclic voltammograms.

Parameter	Value
Scan rate	100 mV/s
Cycles	30
Initial potential	- 0.2 V
Final potential	+ 1.6 V
Step size	10 mV

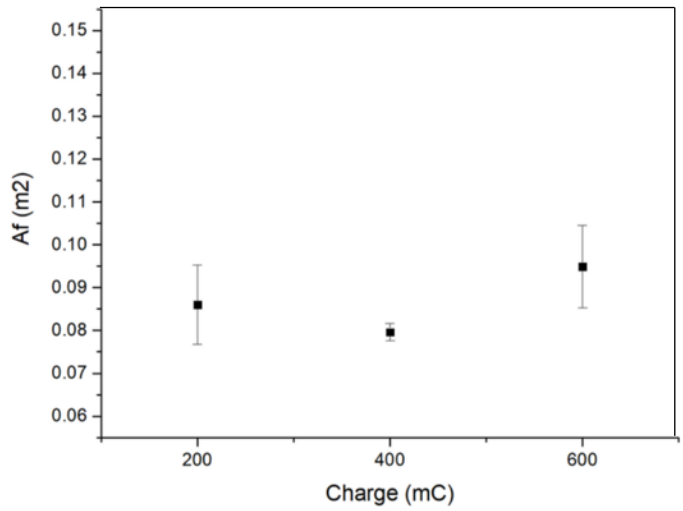

Figure A8 - Average and standard deviation for the results after anodization in 0.3M KCl.

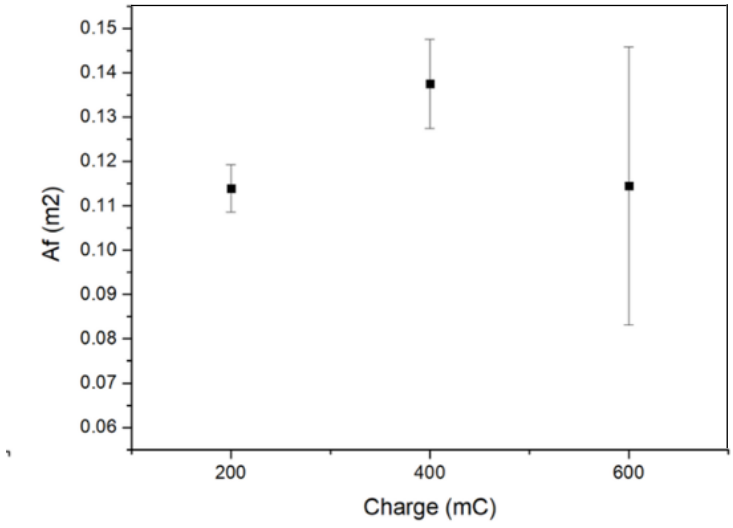

Figure A9 - Average and standard deviation of the results after anodization in 0.5M KCl.

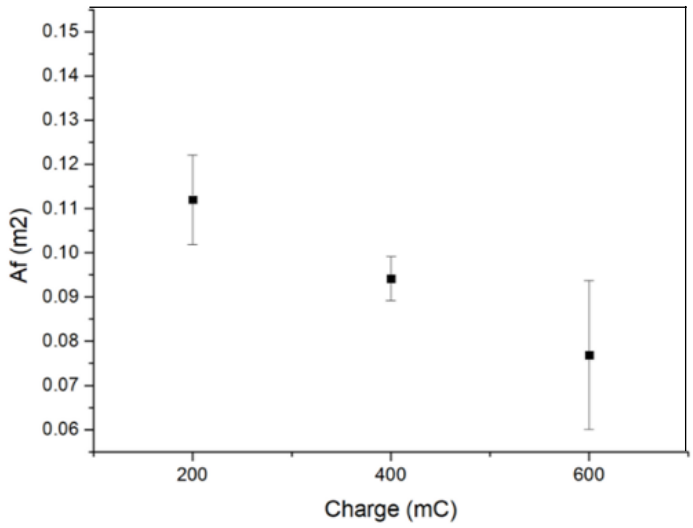

Figure A10 - Average and standard deviation of the results after anodization in 0.7M KCl.

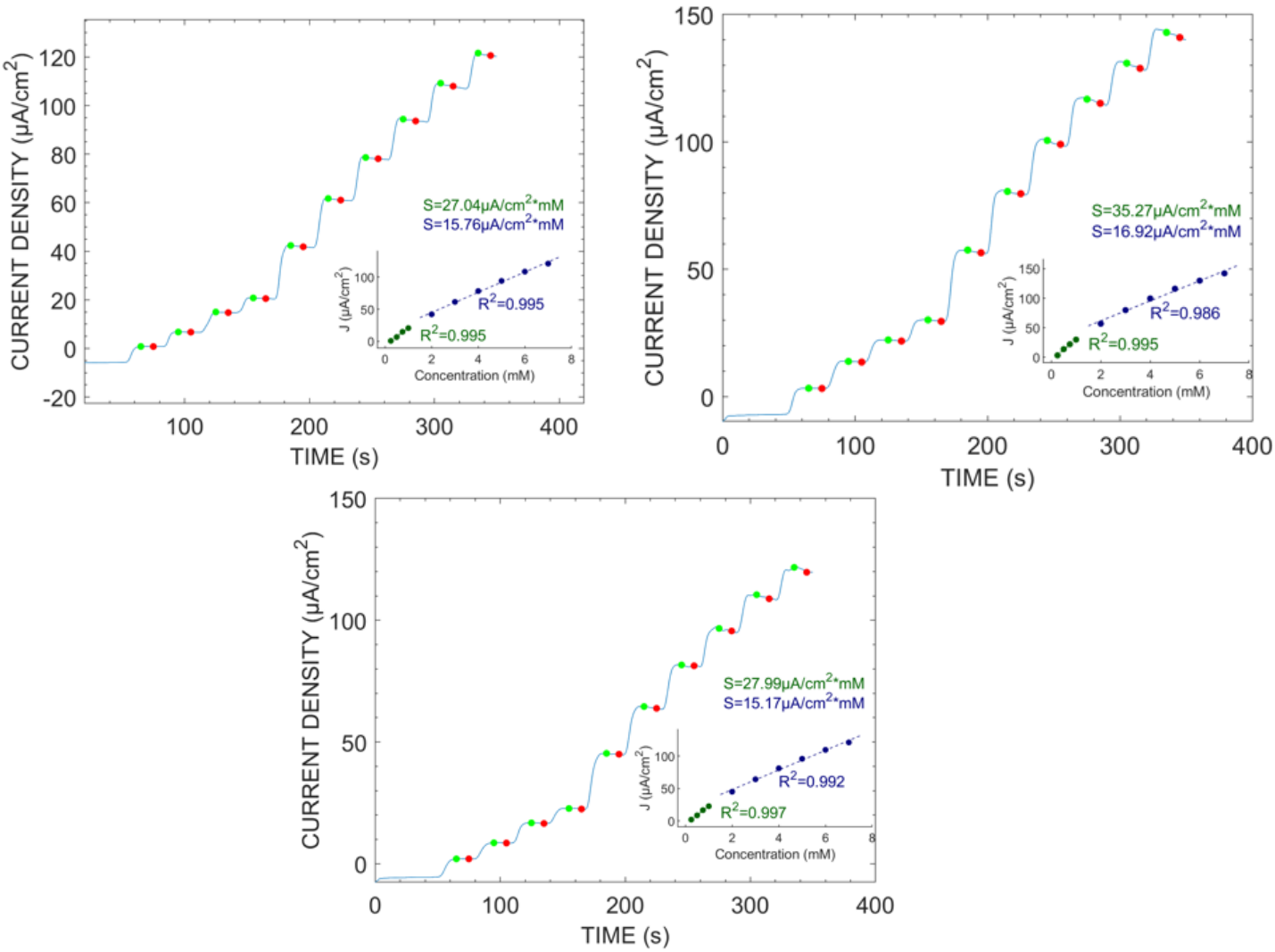

Figure A11 - Chronoamperometry measurement of the nanostructured electrodes in 0.1M PBS at a potential of +0.25V in a stirring condition of 500rpm. Samples were prepared by chronocoulometry in 0.5M KCl applying a charge of 400 mC.

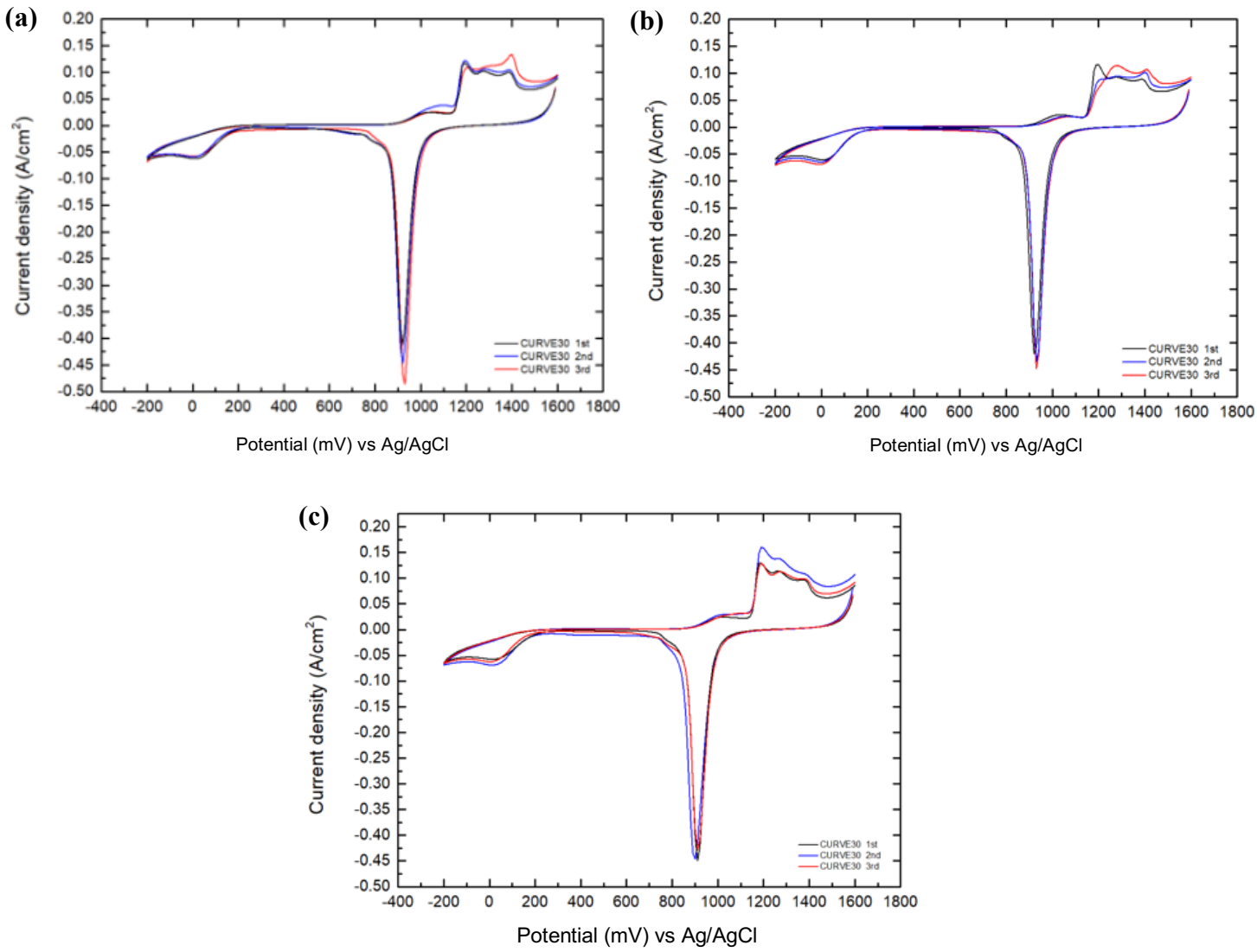

Figure A12 - CVs recorded in 0.5M H_2SO_4, at a scan rate of 100 mV/s and a step size of 10 mV. Signals correspondent to the three samples for each condition. NPG prepared by chronocoulometry in 0.3M KCl where the applied charge was: (a) 200 mC, (b) 400 mC, and (c) 600 mC.

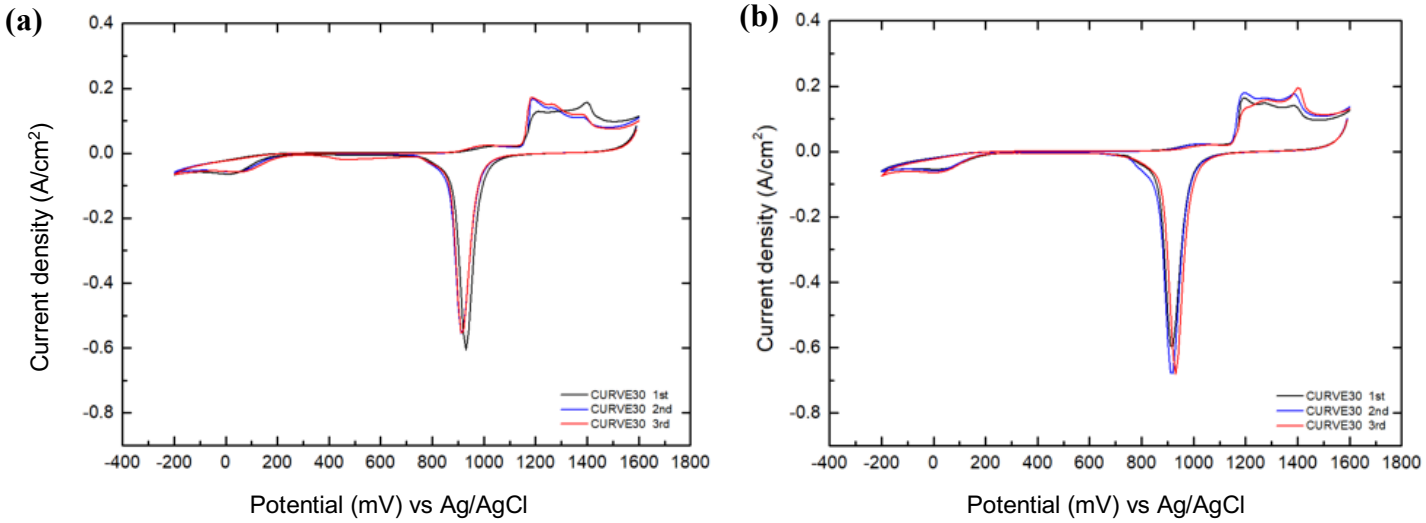

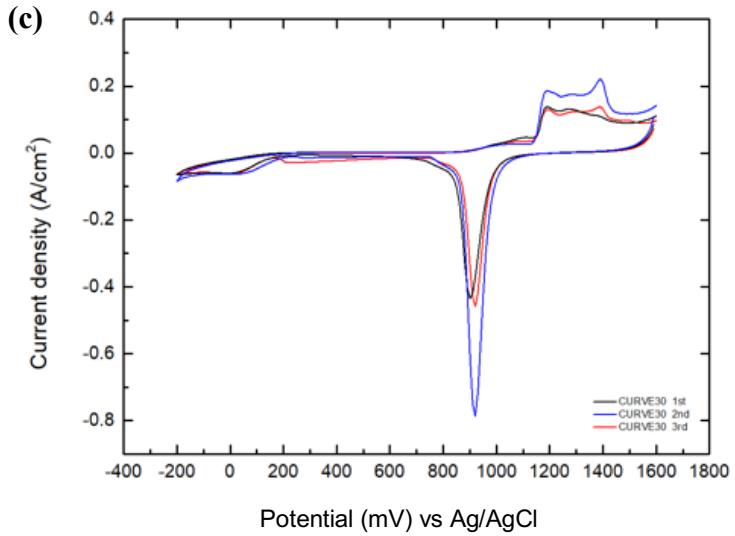

Figure A13 - Cyclic voltammograms recorded in 0.5M H_2SO_4, at a scan rate of 100 mV/s and a step size of 10 mV. Signals correspondent to the three samples for each condition. NPG prepared by chronocoulometry in 0.5M KCl where the applied charge was: (a) 200 mC, (b) 400 mC, and (c) 600 mC

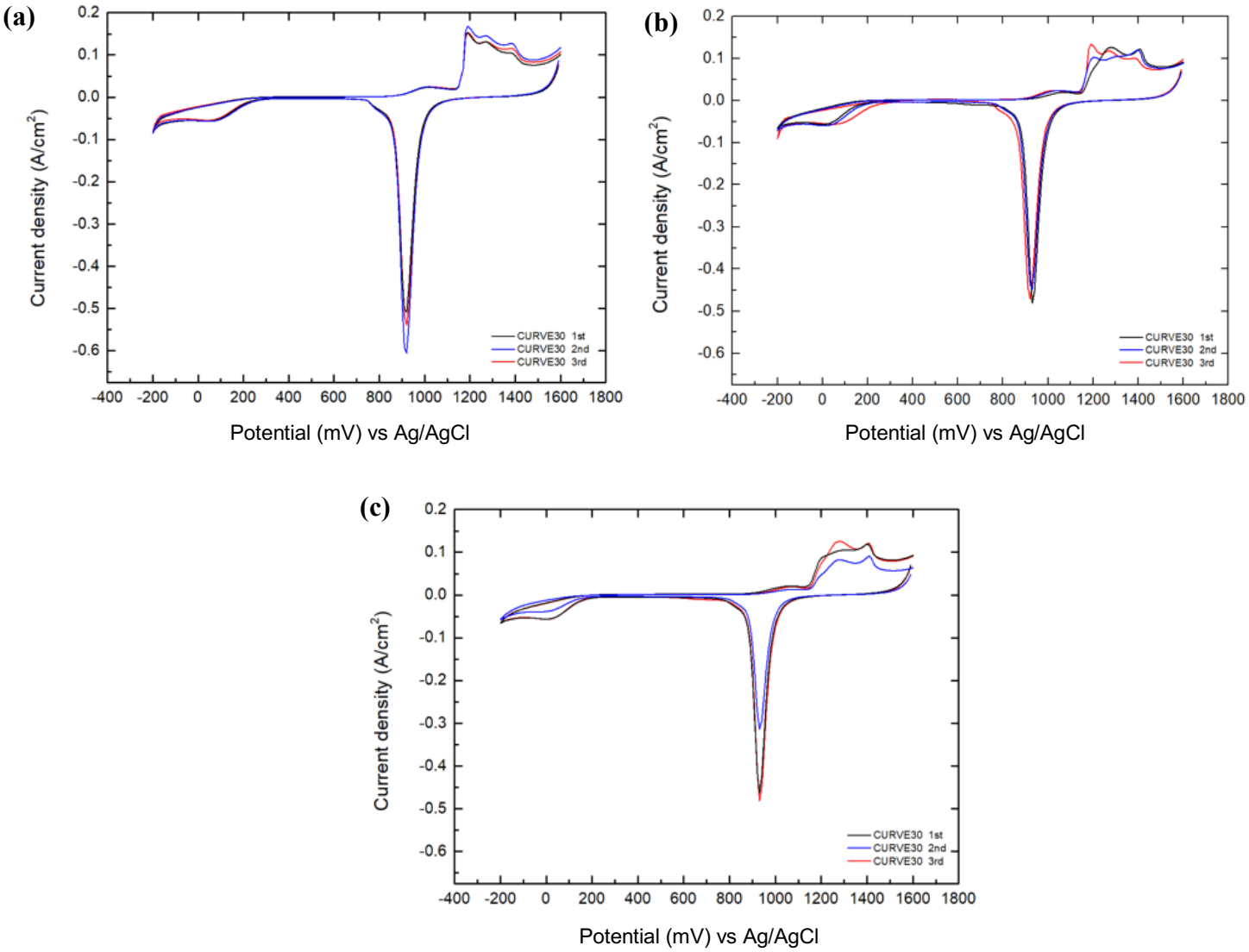

Figure A14 – CVs recorded in 0.5M H_2SO_4, at a scan rate of 100 mV/s and a step size of 10 mV. Signals correspondent to the three samples for each condition. NPG prepared by chronocoulometry in 0.7M KCl where the applied charge was: (a) 200 mC, (b) 400 mC, and (c) 600 mC.